Electrical Characterization of deep levels in Indium Phosphide

By

SEHRISH KHAN

Department of Physics
Quaid-i-Azam University
Islamabad, Pakistan
2011

IN THE NAME OF ALLAH

THE MOST BENEFICIENT

THE MOST MERCEFUL

Electrical Characterization of deep levels in Indium Phosphide

Islamabad

A DISSERTATION SUBMITTED TO THE DEPARTMENT OF PHYSICS, QUAID-I-AZAM UNIVERSITY, ISLAMABAD, IN PARTIAL FULFILLMENT OF THE REQUIREMENTS FOR THE DEGREE OF

MASTER OF PHILOSOPHY

IN

PHYSICS

BY

SEHRISH KHAN

Supervised

BY

DR. UMER SAEED QURESHI

Department of Physics
Quaid-i-Azam University
Islamabad, Pakistan
2011

Certificate

It is certified that the work contained in this dissertation is carried out and completed under my supervision at department of physics, Quaid-i-Azam University, Islamabad, Pakistan.

Supervised by:

(Dr. Umar Saeed Qurashi)
Assistant Professor
Quaid-i-Azam University
Islamabad,Pakistan.

Submitted through:

(Prof. Dr. S.K Hasanain)
Chairman
Department of Physics
Quaid-i-Azam University
Islamabad, Pakistan.

DECLARATION

I hereby declare that I have worked on my thesis "Electrical Characterization of deep levels in indium phosphide" Independently and the work presented here is original. This thesis has not been submitted in the current or a similar form to any other university.

Sehrish Khan

Islamabad, 2011

Dedicated
to my
Loving and Sweet
Parents

ACKNOWLEDGEMENT

All praises to **Almighty Allah**, Who created us as a Muslim and blessed us with knowledge to differentiate between right and wrong. Many many thanks to Him as He blessed us with the **Holy Prophet, Hazrat Muhammad**  for whom the whole universe is created and who enabled us to worship only one God. He (PBUH) brought us out of darkness and enlightened the way of Heaven.

I feel great pleasure in expressing my ineffable thanks to my encouraging research supervisor Assistant Prof. Dr. Umer Saeed Qureshi whose unique thought provoking guidance, encouragement, valuable suggestions and discussions enabled me to complete this tedious work. It is really an honour for me to be a research student under his kind supervision.

I am thankful to Chairman, Prof. Dr. Khursheed Hasanain, Department of Physics **Quaid-i-Azam University, Islamabad** for providing necessary research facilities. Special thanks are due to all **teachers** for being a source of inspiration and enlightenment for me.

I also owe my recognition to my lab fellows **Aqdas Fareeza, Yaqoob, Rashid Khan, Zafar and Waqas** for their help at crucial times of my research work. Especially to my senior **Aqdas Fareeza** for her advice and guidance in experimental.

I am thankful to all my dear friends specially **Afshan Niaz, Humaira Zafar, Mudassir zahra, Kalsoom Chishti, Areeba Sadiq, Hafiza Fizzah Riaz** and all others for care and providing a relaxed environment during my work.

Many thanks are due to the supporting staff of the department, for their all time help.

I have no words to acknowledge the sacrifices, efforts, lot of prayers, guidance, support, encouragement and firm dedication of my Sweet **parents.** Their endless prayers contributed to the successful completion of this research project.

Loving thanks from the core of my heart to my sister **Ayesha** and brothers, **Ziaullah Khan, Saifullah Khan, Abbas Khan** for very much care and love in my thesis write up. May God give them success always.

Sehrish Khan

CONTENTS

LIST OF GRAPHS

LIST OF FIGURES

ABSTRACT

Deep levels in Iridium doped n-type InP grown by Metal Organic Chemical Vapour Deposition (MOCVD) technique has been studied using Deep Level Transient Spectroscopy (DLTS). The basic working principal of DLTS is changing the occupancy of deep levels by changing the reverse bias of the P-n junction. When p-n junction is reversed biased, depletion region width increases and junction capacitance decrease. Applying the reverse or the forward bias pulse to the sample, the deep levels are filled with the carriers and become empty if sufficient thermal energy is available. The change in capacitance of the junction due to emission of the carriers gives rise to capacitance transient.

No deep level is observed in minority carrier spectra of n-type InP. The majority carrier emission spectra are found to be much more richer i-e six electron – emitting levels in n-type Iridium doped Indium Phosphide. Six electron emitting deep levels in Iridium doped Indium Phosphide at 500μsec pulse width are obtained. P0 is overlap of two peaks, one with activation energy 0.22eV with error ±0.02 and other with activation energy 0.09eV with error ±0.04. P1 is also overlap of two peaks, one with activation energy 0.28eV with error ±0.03 and other with activation energy 0.19eV with error ±0.02. P2 is overlap of two peaks one with activation energy 0.14eV with error ±0.09 and other with activation energy 0.22eV with error ±0.01. The activation energy of P3 is 0.38eV with error ±0.02, P4 is 0.53 with error ±0.02, P5 is 0.51eV with error ±0.004and P6 is 0.52eV with error ±0.001. Capture cross section of highest two levels are also found. The data for P4 shows a sum of two exponentials giving two values of capture cross section $\sigma 1 = 2.19\times10^{-22}cm^2$ and $\sigma 2 = 1.41\times10^{-22}cm^2$.The data for P5 shows the sum of three exponentials giving three capture cross sections $\sigma 1 = 1.97\times10^{-22}cm^2$, $\sigma 2 = 6.64\times10^{-22}cm^2$ and $\sigma 3 = 8.56\times10^{-22}cm^2$.

CHAPTER 1

INTRODUCTION

A semiconductor is a material with electrical conductivity due to electron flow (as opposed to ionic conductivity) intermediate in magnitude between that of a conductor and an insulator. This means conductivity is roughly in the range of 10^3 to 10^{-8} siemens per centimeter. Semiconductor materials are the foundation of modern electronics, including radio, computers, telephones, and many other devices. Such devices include transistors, solar cells, many kinds of diodes including the light-emitting diode, the silicon controlled rectifier, and digital and analog integrated circuits. Solar photovoltaic panels directly convert light energy into electrical energy. In a metallic conductor, current is carried by the flow of electrons. In semiconductor, current is often schematized as being carried either by the flow of electrons or by the flow of positively charged "holes" in the electron structure of the material. Actually, however, in both cases only electron movements are involved.

Common semiconducting materials are crystalline solids, but amorphous and liquid semiconductors are known. These include hydrogenated amorphous silicon and mixtures of arsenic, selenium and tellurium in a variety of proportions. Such compounds share with better known semiconductors intermediate conductivity and a rapid variation of conductivity with temperature, as well as occasional negative resistance. Such disordered materials lack the rigid crystalline structure of conventional semiconductors such as silicon , which are less demanding as far as is concerned the electronic quality of the material and thus are relatively insensitive to impurities and radiation damage. Organic semiconductors, that is, organic materials with properties resembling conventional semiconductors, are also known.

Silicon is used to create most semiconductor devices commercially. Dozens of other materials are used, including germanium, gallium arsenide and silicon carbide. A pure semiconductor is often called an intrinsic semiconductor. The electronic properties and conductivity of a semiconductor can be changed in a controlled manner by adding very small quantities of other elements called "dopants" to the intrinsic material. In crystalline silicon this is achieved by adding impurities of boron or

phosphorous to the melt and then allowing the melt to solidify into the crystal. This process is called "doping".

1.1 III-V Compound semiconductors

III-V compound semiconductors are binary crystals with one element from the metallic group III of the periodic table, and one from the non-metallic group V. The family includes GaAs, InP, GaN, InSb and InAs and many others. Some of these binary compounds are known for their high mobility of electrons and holes, which in the case of the best known example, Gallium Arseneid facilitates the operation of reasonable high speed devices. Bandgap in III-V semiconductors is greater than that of elemental semiconductors. Some of them are direct bandgap materials. Due to this direct band gap they have greater carrier mobility. The lifetime of direct band gap material is usually smaller than indirect band gap materials.

Varying the percentage of any one of two elements in a binary compound, one can vary the bandgap in III-V semiconductors. They also have low effective mass of electron in Γ-valley, resulting in low resistivity e.g. InP, GaAs, BN, BP, BaS, AlN, AlP, AlSb, GaN, GaP InN, InAs and InSb. All except nitride compounds crystallize into the Zinc Blend structure. Nitrides are stable in Wurtize structure. BN and GaN also have metastable Zinc Blend phase [14]. The principal application of III-V semiconductors and their alloys lie in the field of optoelectronic like LEDS, photo diodes for optical fiber communication and laser diodes. Some general properties of III-V semiconductors are listed below.

Some of III-V semiconductors are used in high-speed devices. The power dissipation is also low in these III-V semiconductors. So these are used in communication and optical fiber industry.

(a) The tolerance, hardness and operation of III-V semiconductors are wide over long range of temperature.

(b) InP is commonly used as substrate for epitaxial InGaAs. It has superior electron velocity, used in high-power and high-frequency applications. Used in optoelectronics.

(c) $Al_xGa_{1-x}As$, can be lattice-matched to GaAs substrate over entire composition range; tends to oxidize; n-doping with Si, Se, Te; p-doping with Zn, C.

(d) We can easily form their ternary compound by using Molecular Beam Epitaxy (MBE), Vapour Phase Epitaxy (VPE), Liquid Phase Epitaxy (LPE) and Metal Organic Chemical Vapour Deposition (MOCVD) techniques. By the use of these techniques, quantum dots, quantum wires, quantum wells and high electron mobility transistors can be grown. III-V semiconductor quantum-wire structures are grown by solid and gas source molecular beam epitaxy [12].

1.2 Indium Phosphide

Indium Phosphide is a III-V semiconductor. Its crystalline structure is Zinc Blend as shown in Fig. 1.1. Its dielectric constant is 12.56 and lattice parameter of InP is 5.86 A°. All atoms form tetrahedral covalent bond having sp^3 hybridization. One atom of Indium is surrounded by four atoms of Phosphorous and vice versa.

Indium from group III is a metal. $_{49}In^{114.82}$ having electronic configuration $4d^{10}5s^25p^1$. It has only one natural isotope. Phosphorous from group V is $_{15}P^{30.97}$ having electronic configuration $3s^23p^3$. It is non-metal and has no natural isotope.

The first Brillion zone of Indium Phosphide is shown in Fig.1.2. It is the Wigner- Seitz cell in reciprocal lattice. Wigner –Seitz cell is the smallest polyhedron enclosed by the perpendicular bisectors of the nearest neighbors of lattice. The first Brillion zone of Indium Phosphide is a truncated octahedron, i.e. a regular octahedron with the tips in the direction of three perpendicular axes cut off forming squares [9]. Indium Phosphide is a direct band gap material having band gap 'E_g' of 1.34eV. Direct band gap means that a conduction band minimum lies directly above the valance band maxima in momentum space as shown in Fig. 1.3. A direct band band gap material can emit light whereas an indirect band gap material cannot do so competently. This means that the quantum transitions , which takes place when a photon is emitted or absorbed , do not require any change in the momentum of carriers,i.e. they occur much more readily , making the material highly suitable for fabricating devices such as lasers and LEDs. This direct band gap supports optical

gain as required for lasers, and also very high absorption (photons can be absorbed within very short distance) making functions such as data modulators or fast photo-detectors easy to implement.

Since the electronic properties of a semiconductor are dominated by the outermost partially empty band and the lowest partially filled band. It is often sufficient to consider those bands. This leads to simplified energy band diagram for semiconductors.

1.2 Energy Band Structure of Indium Phosphide

With the help of E-k relationship where "E" is the energy and "k" is wave vector one can obtain a lot of information about a semiconductor. The energy band diagram of semiconductors are rather complex. The energy is plotted as a function of the wave vector "k" along the main crystallographic axes and direction in a crystal, because the band diagram depends on the direction in the crystal. The energy band diagram contains multiple filled and completely empty bands.

Bandgap is the energy difference between the top of the valance band and the bottom of the conduction band. Indium Phosphide valance band maxima and conduction band minima has direct band gap along "Γ-valley" is 1.34eV at origin (000), band gap along "L-valley" is 1.93eV along <111> direction with respect to valance band and along "X-valley" is 2.19eV along <100> direction with respect to valance band maxima as shown in Fig.1.3.

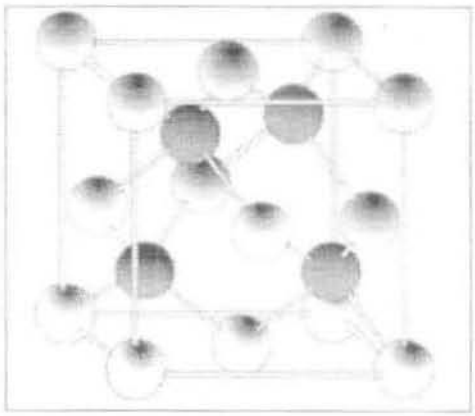

Fig.1.1: Zinc Blend crystal structure of Indium Phosphide

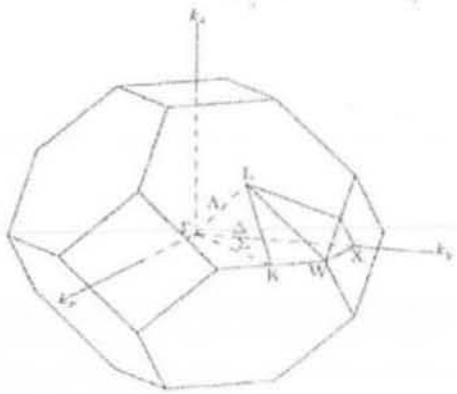

Fig 1.2 First Brillion zone of Indium Phosphide and its important crystal directions

Γ-(000)--zone center

L-(111)--and 7 other equivalent points

X-(100)--and 5 other equivalent points

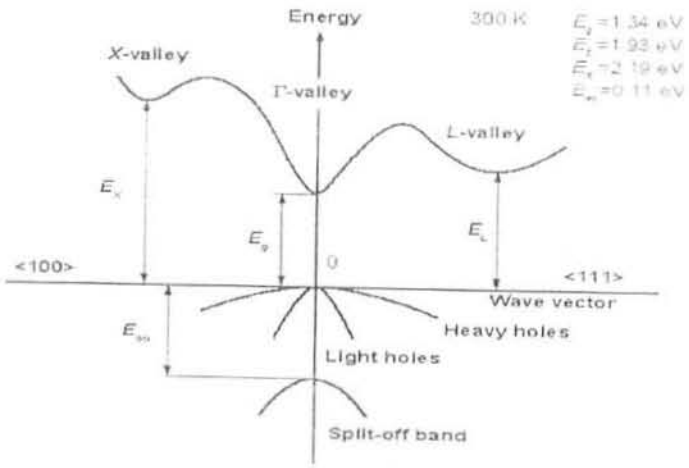

Fig 1.3: Important minima of the conduction band and maxima of the valence band at 300 K of Indium Phosphide

1.4 Motivation of the Present research work

The III-V semiconductors GaAs, GaN, InP and AlP are one of the most important semiconductors. Indium Phosphide is one of the III-V semiconductors undergoing strong research and development. These are presently called next generation compounds. One important reason for this interest is the promise of this material for high efficiency solar cells and its much higher resistance to radiation in space compared to Si and other compound semiconductors.

InP pn-junctions grown using MOCVD technique has its own importance. In the present research work we characterized the InP grown using MOCVD by Deep Level Transient Spectroscopy. Deep level Transient Spectroscopy (DLTS) is a very resourceful technique for the determination of nearly all parameters connected with traps including concentrations, thermal activation energy, capture cross section and depth profile. Very little work has been done on Iridium doped. This provides the basic motivation for the present research study.

CHAPTER 2

KINETICS OF DEEP LEVELS

This chapter describes the crystal defects, generation –recombination kinetics are discussed in terms of Shockley-Read-Hall Theory. The electrical parameters, usually used to illustrate a deep level are discussed. The shallow levels are also discussed to some extent. At the end, trapping and recombination processes via the deep levels are briefly explained.

2.1 Crystal defects in semiconductors

Defects in semiconductor material play a very important role in the understanding of their electrical and optical properties. As a result of early experiments, semiconductors were viewed as family of solids with irreproducible properties due to high density of unwanted defects. Research in semiconductor defects overcame this problem and successfully turned the art of impurity doping and material fabrication into today's extremely useful and reproducible technology that is used to control specifically electrical conductivity, composition and minority carrier lifetime over wide ranges.

Crystal defects can be classified according to their dimensions into following categories.

1. Zero-Dimensional defects (0-D)

2. One-Dimensional defects (1-D)

3. Two-Dimensional defects (2-D)

4. Three-Dimensional defects (3-D)

2.1.1 Zero-Dimensional defects

Zero dimensional defects are also termed as "Point defects" or "atomic size defects". Point defects are located at a given atom in the lattice and involve their immediate adjoining neighbors. Their size is of the order of atomic dimension. Point defects are single atom or vacancy present in a crystal lattice, which are briefly explained as below.

(a) Vacancy

A vacancy is created when an atom moves out of its regular site. If an atom migrates from its regular site to the surface of the crystal and settles there at a lattice site, the defect is known as the Schottky defect. If there are 'N' atoms and 'n' number of vacancies in equilibrium for n < N then the concentration of vacancy is given by

$$n = N \exp\left[\frac{-E_a}{K_B T}\right] \qquad 2.1.1$$

Where E_a is the energy required to take an atom from inside the lattice site on the surface. T is absolute temperature and K_B is Boltzmann constant.

Another vacancy defect is the Frenkel defect in which an atom is transferred from a lattice site to an interstitial position. If 'n' is the number of Frenkel defect, is smaller than the number of lattice sites N and number of interstitial sites in thermodynamic equilibrium 'N_{qqq}' then concentration of vacancy is given

$$n = NN_{\circ} \exp\left[\frac{-E_a}{K_B T}\right] \qquad 2.1.2$$

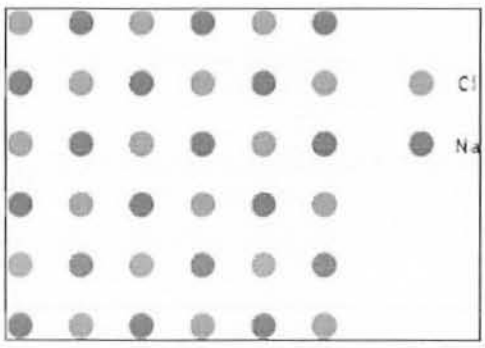

Fig. 2.1.a NaCl crystal

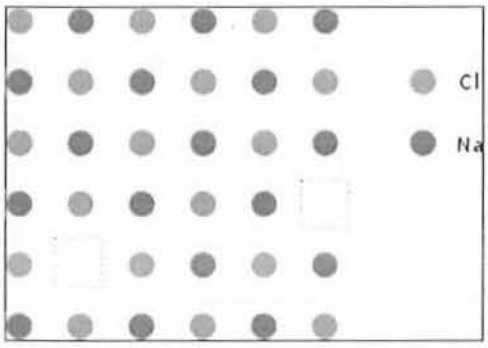

Fig. 2.1.b Schottkey defects in NaCl

(b) Interstitial Defect

Interstitials are atoms which occupy a site in the crystal structure at which there is usually not an atom. They are generally high energy configurations. Small atoms in some crystals can occupy interstices without high energy.

(c) Antisite Defect

If a crystal consists of two different chemical elements then an atom of first may occupy the position of the second and vice versa. Antisite defect occur in an ordered alloy in which two species atoms A and B mutually exchange their position. This is neither a vacancy nor an interstitial, nor an impurity.

(d) Substitutional Defect

When a foreign impurity atom substitutes an atom of the host crystal then it forms substitution defect i.e those impurities in which a foreign impurity atom is occupying an atomic lattice site. This is neither a vacant site nor is the atom on an interstitial site.

(e) Self-Interstitial Defect

If a chemically correct atom of the crystal occupies an interstitial site rather than regular one, it is called self-interstitial.

2.1.2 One-Dimensional defects

This includes all kinds of dislocations, also termed as line defects, which often extend throughout the entire lattice. There are two main types of dislocations

a) Edge dislocation

b) Screw dislocation.

(a) Edge dislocation

Edge dislocation can be thought of as resulting either from the presence of an extra plane of atom or of a missing plane of atoms in the structure as shown in Fig2.2.In either case, an extra plane of atoms does not extend throughout the entire crystal but instead terminates within the crystal. The edge dislocation is considered to be localized in the region around the line at the end of the extra plane of atoms where the deviation of atoms from their normal position is greatest. This line is the dislocation line, and the region surrounding it is the dislocation core.

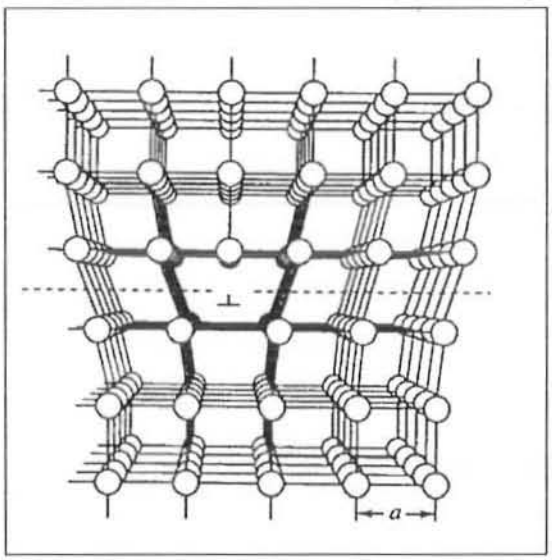

Fig. 2.2 Edge dislocation; the atom positions around an edge dislocation; extra half –plane of atoms shown in perspective

(b) Screw dislocation

The screw dislocation is formed by a shear stress which causes, one side of the crystal to be shifted by a lattice constant relative to the other side as shown in fig2.3. The term screw dislocation refers to the fact that the originally parallel planes in the crystal are now joined by a spiral or helical path. Dislocations can also form closed paths within the crystal, in which case they are called dislocation loops.

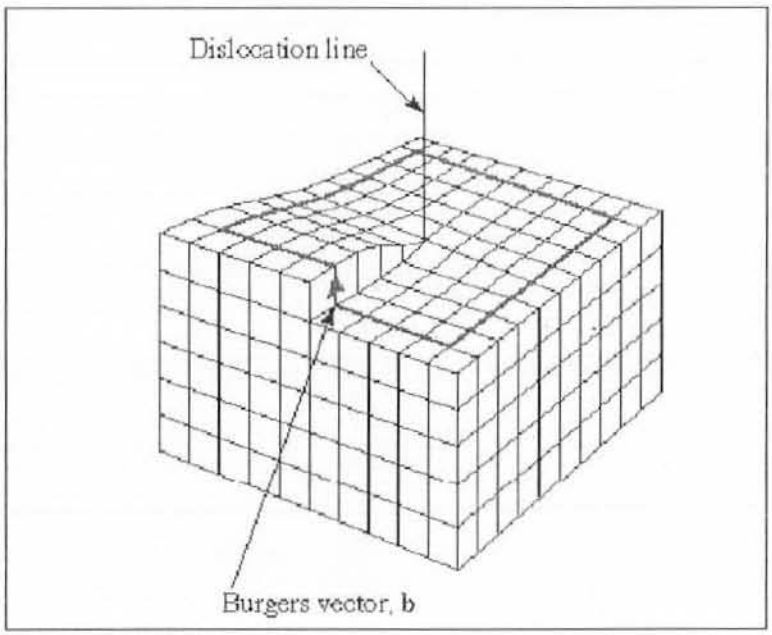

Figure 2.3 screw dislocation

2.1.3 Two -Dimensional defects

Staking faults (SF), Twin boundaries' (TB), Grain Boundaries (GB), Sub boundaries (SB) and surfaces are typical examples of two- dimensional defects in crystals. Such defects are also known as surface defects or planer defects. These defects have significant influence on the electrical and optical properties of semiconductors. Most of this influence is caused by the defect levels at the boundaries of the semiconductors which are charged and attract compensating charges in the adjacent space charge of the crystal.

2.1.4 Three Dimensional Defects

This includes precipitates, usually involving impurity atoms, voids (little hole, i.e., agglomerates of vacancies in three- dimensional form) which may or may not filled with a gas special defect e.g. stacking faults tetrahedron and tight clusters of dislocation. Such defects are also referred to as volume defects.

2.2 Shallow and deep levels

In semiconductors there exist two types of electrically active defects, namely shallow levels and deep levels. The term shallow and deep level is due to their position in energy with respect to the conduction or valance band.

2.2.1 Shallow Levels

Shallow impurities are impurities which require little energy-typically around the thermal energy or less to ionize. Shallow levels are those energy levels introduced by impurity atoms inside energy band gap at energy less than 50meV from the conduction or valance band edge. This energy can be described adequately by hydrogenic effective mass theory i.e. hydrogen-like model. These levels have very low activation energy (<0.1ev), commonly shallow levels are obtained by adding an impurity atoms which has, in its outermost shell, one electron in excess or one electron less than in the host atoms electronic configuration. These impurity atoms are frequently of the same size as host atoms. As an example, shallow donors and acceptors can be formed by the substitution of group V and III elements in Silicon ,respectively.

These levels are ionized at room temperature and provide charge carriers in valance band to make it p-type or to make it n-type. For donors this implies that the electron density equals the donor concentration, or:

$$N_d^+ \cong N_d$$

While for acceptors the hole density equals the acceptor concentration, or:

$$N_a^- \cong N_a$$

Most important role of shallow levels is to control electrical conductivity of semiconductors because their ionization energy is comparable to k_BT at room temperature so that these levels are completely ionized at room temperature and contribute to electrical conductivity.

2.2.2 Deep levels

These energy levels are introduced by impurity or structural defects in forbidden gap that cannot be described adequately by hydrogen effective mass theory. They are created from defect centers in which their core potential play a dominant role. If the defect in semiconductor is not belonging to the adjacent group of periodic table then they form deep levels. Their ionization energy is greater than 50meV from valance band edge or conduction band edge, so they are not ionized at room temperature and hence do not contribute in conduction.

They generate the bound states with well localized wave functions. These defects are called deep or localized levels. They can act as recombination-centers or deep level traps. Thus they limit the lifetime of the carrier and may compensate the shallow donors or acceptors or they may introduce the pinning of the Fermi level. Their energy level lie 'deep' within the forbidden energy band and are much more difficult to understand then the Shallow level defects [16,2]. Improper placing of impurity atoms distorts the host lattice extensively that binding energy greatly exceeds the Shallow hydrogenic defects. Presence of deep levels can produce efficient radiative recombination, even in materials with indirect band gap. So deep levels can

be useful to the working of device. Presence of deep levels could increase the leakage current of a device.

Deep levels are "connected" to the conduction and valance bands and often provide preferred path for carrier recombination or act as deep traps. When an impurity level acts as trap or generation recombination center, it depends on the location of the Fermi level in band gap, the temperature and capture cross-section of the carrier. Those impurities whose energies lie near the middle of the band edges acts as traps [10].

2.2.3 Role of deep levels in semiconductors

Electrical properties such as mobility, resistivity and carrier lifetime of semiconductors are very sensitive to the presence of deep levels. They act as recombination centers when there are excess carriers in the semiconductors and as generation centers when carrier density is below its equilibrium values in reverse biased pn-junction or Metal Oxide Semiconductor (MOS) capacitors [7].

Resistivity of a semiconductor can be increased by the process of compensation e.g. the controlled addition of deep acceptor state in n-type semiconductor. Thus high resistivity materials can be produced by an appropriate addition of deep level in a given semiconductor. In some semiconductors like GaAs and InP, deep level impurities raise the substrate resistivity to form semi-insulating substrate. So deep levels play an important role in semiconductors.

2.3 Deviation from Equilibrium

Carrier injection is a phenomenon where excess charge carriers are introduced within a semiconductor under non-equilibrium conditions, usually through optical and electrical excitation. A semiconductor is put in non-equilibrium if an external agent such as voltage, current, electric field, or light is applied to it. For instance if an electric field is applied to a semiconductor, both electron and hole-concentration will change. A study of the behavior of excess carrier is important because most of the semiconductor devices operate under nonequlibrium conditions in which the electron and hole concentrations are significantly different from their thermal equilibrium

values. It is the process of injection and extraction of minority carriers in a semiconductor in which the equilibrium condition $np=n_i^2$ is violated [3].

There could be two types of deviations

1. In which $np>n_i^2$ we call it injection of carrier

2. When $np< n_i^2$, we call it the extraction of carriers from semiconductor

(a) Low level Injection

A process by which excess carriers are introduced into a semiconductor. With carrier injection, np becomes greater than the n_i^2, with the increase in the minority carriers being much more prominent than the increase in majority. The condition where the excess carrier concentration is negligibly small in comparison to the doping concentration i.e. $\Delta p=\Delta n \ll N_d$ is referred to as low- level injection.

(b) High–level injection

In this case the excess carriers are large or at least comparable to the concentration of donor or acceptor ions. Thus in this case the percentage change in majority carrier is no longer negligible. Even though high level injection is also encountered in semiconductor device operation, but because of the complexities involved in its treatment, we only consider low- level injection. If the external agent that put the semiconductor in non-equilibrium is removed, the carrier concentration will decrease exponentially to return to their thermal equilibrium levels.

2.4 Return to equilibrium

Whenever carrier concentration is disturbed from their equilibrium values, they will attempt to attain equilibrium. In case of injection of the carriers, return to equilibrium takes place through recombination. In the case of extraction of the carriers return to equilibrium is through the process of generation of electron-hole pairs.

2.5 Kinetics of Generation-Recombination Processes

The rate of return of the minority carrier distribution to equilibrium depends on the rate constant which characterizes the recombination process is given by the relation $1/\tau_p$. Recombination of electrons and holes is a process by which both carriers annihilate each other: electrons occupy through one or multiple steps- the empty state associated with a hole. Both carriers eventually vanish in the process. The energy difference between the initial and final state of the electron is released in the process. This leads to one possible classification of the recombination processes. These processes are further illustrated in Fig.2.4.

In some states, the generation and recombination of electron-hole pairs are in equipoise. The number of electron-hole pairs in the steady state at a given temperature is determined by quantum statistical mechanics. The precise quantum mechanical mechanics of generation and recombination are governed by conservation of energy and conservation of momentum. As the probability that electrons and holes meet together is proportional to the products of their amounts, the product is in steady state nearly constant at a given temperature, provided that there is no significant electric field or externally driven pair generation. The product is a function of the temperature, as the probability of getting enough thermal energy to produce a pair increases with temperature, being approximately $\exp(-E_G/kT)$, where k is Boltzmann's constant, T is absolute temperature and E_G is band gap.

2.5.1 Band to Band Transition

In band-to-band transition electrons in the conduction band and holes in the valence band recombine directly as depicted in Fig.2.4. In such a recombination the electron loose energy of the order of the band gap, this is emitted in the form of light or heat. In direct band gap materials, the excess energy of the electron-hole pair recombination is released as a photon of light instead of the less likely process of heat generation. This radiative transition then conserves energy and momentum by giving light whenever an electron and hole recombine. This gives rise to a new type of device, the light emitting diode (LED). In case of indirect band gap material, in band-

to-band transition when an electron goes from the bottom of the conduction band to the top of valance band, it must also undergo a significant change in the momentum.

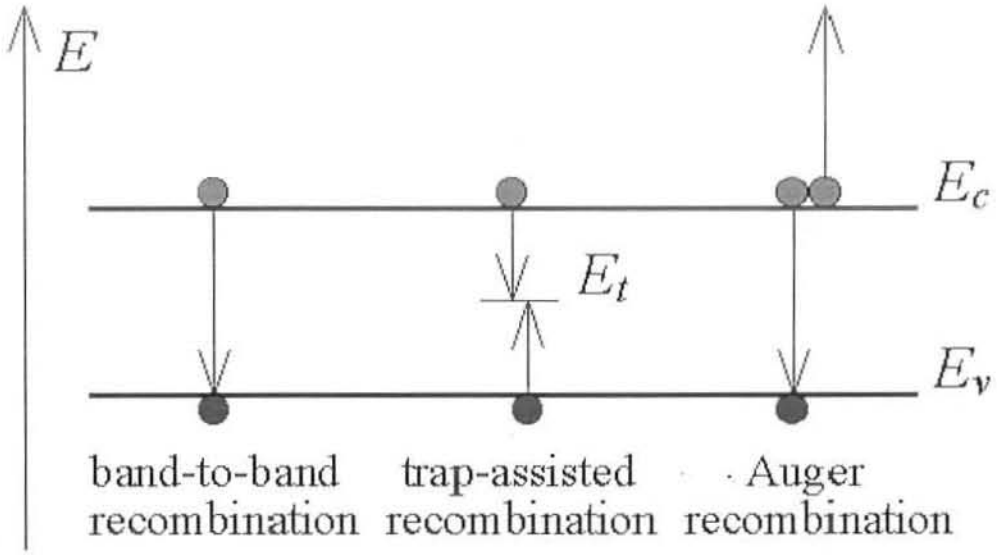

Fig. 2.4 Recombination pocesses

2.5.2 Recombination-Generation through Intermediate Centre

Sometimes impurities introduce deep levels in the forbidden region inside band gap, similar to those like donors and acceptors. These energy levels then act as stepping-stones in transition of electrons and holes between the conduction and valance band. The probability of transition depends on the size of the step and imperfection can make such transition more probable. Hence these stepping –stones have a drastic influence on the lifetime of semiconductors.

2.5.3 Auger recombination

Auger recombination is a process in which an electron and a hole recombine in a band-to-band transition, but now the resulting energy is given off to another electron or hole. The involvement of a third particle affects the recombination rate so that we need to treat Auger recombination rate differently from band-to-band recombination.

2.5.4 Generation mechanism

Each of these recombination mechanisms can be reversed leading to carrier generation rather than recombination. In addition, there are generation mechanisms, which do not have an associated recombination mechanism: generation of carriers by light absorption or a high energy electron/particle beams. These processes are referred to ionization processes. Impact ionization, which is the generation mechanism, associated with Auger recombination also belongs to this category.

2.6 Kinetics of deep Levels and Shockley, Read and Hall theory

Impurity atoms other than donor and acceptors and some types of crystal defects in a semiconductors, introduced localized energy levels deep in the band gap away from the band edges. These levels act as stepping stones for electrons between the conduction and valance band, making a substantial enhancement in the recombination process. Depending on its location in the band gap, a deep level may act as an electron or a hole trap or a recombination centre. An electron trap has a high probability of capturing a conduction electron and setting it free after sometime. Similarly, a hole trap has a high probability of capturing a hole that is subsequently released into the valance band. At a recombination center the probabilities of electron and hole capture are nearly equal. Thus an electron capture is followed by a hole capture, and this results in the elimination of an electron-hole pair. The mechanism of indirect recombination through the deep level centers has been investigated by Shockley , Read [18] and Hall [13].

2.6.1 A Pictorial view

To follow the various capture and emission processes, let the centre first capture an electron from the conduction band, shown in Fig.2.5 (a) The two mechanisms of recombination in a semiconductor (a) Band-to-Band recombination and (b). Recombination via some intermediate state such as a deep level at E_t perturbed by foreign atoms or crystal defects, discrete energy levels are introduced into band gap, shown by E_t lines in Fig.2.5 and characterized by capture coefficient C_n. After electron capture, one of two events takes place. The center can emit the

electron back to the conduction band called electron emission e_n as shown in Fig. 2.6(a), or it can capture a hole from the valance band called hole capture c_p as shown in Fig. 2.6(d).After either of these events, the G-R (generation- recombination centers) is occupied by hole and again has two choices, either it emits the holes back to the valance band called hole emission e_p as shown in Fig.2.6(c) or capture an electron called electron capture c_p as shown in Fig.2.6(b).

A recombination event is Fig.(b) followed by Fig.(d) and generation events is Fig.(a) followed by Fig.(c). A third event, that is neither recombination nor generation, is the trapping event. In which a carrier is captured, subsequently is emitted back to the band from where it came. Only one of the two bands and center participate and the impurity is a trap. Whether an impurity acts as a trap or a G-R center depends on the location of Fermi level in the band gap, the temperature, and the capture cross section of the impurity. These impurities whose energy lie near the middle of the band gap behave as G-R centers, where as those near the band edges act as traps.

Generally, the electron emission rate for centers in upper half of the band gap is much higher than the hole emission rate. Similarly the hole emission rate is generally much higher than electron emission rate for centers in the lower half of the band gap. For most centers one emission rate dominants and the other can frequently be neglected.

2.6.2 A Mathematical view

An electron-hole pair can combine in two ways; either an electron jumps directly from the conduction band and combines with a hole in the valance band or an electron from conduction band reaches a hole in the valance band through a step as shown in Fig.2.6, Schokely, Read and Hall worked out the theory of indirect recombination. According to which if a level is present in the band-gap then four basic emission and capture processes can take place as shown in Fig.2.6.

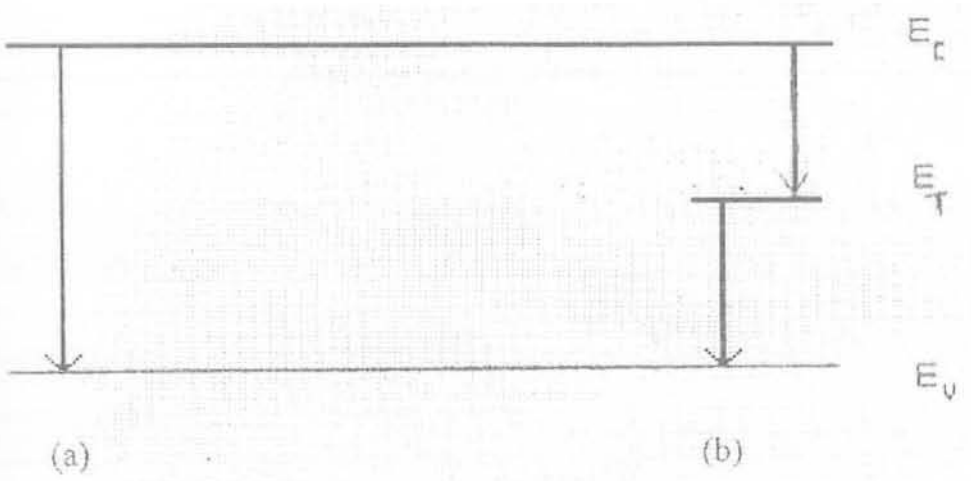

Fig 2.5 The two mechanisms of recombination in a semiconductor. (a). band -to-band recombination and (b). recombination via some intermediate state such as a deep level at E_T

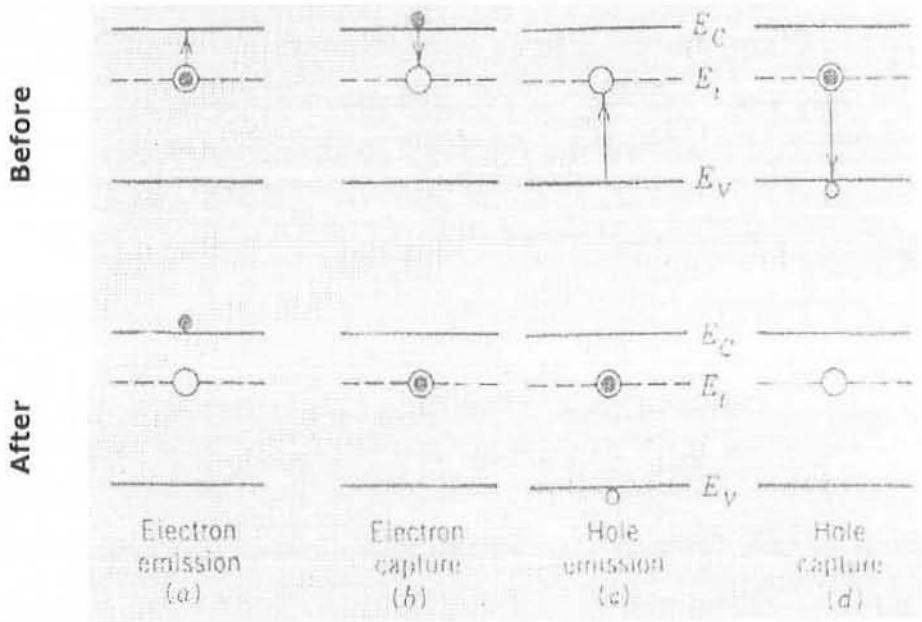

Fig. 2.6. The four steps that occur in recombination of an electron – hole pair through level centre. The arrow indicates the transition of the electron in the process.

Process 1

Emission of electrons from a deep level to conduction band. The rate of electron emission 'R1' is described by

$$R_1 = e_n n_T \qquad (2.1)$$

Where 'e_n' is proportionality constant and defines as the electron emission rate and n_T is the density of filled traps.

Process 2

Capture of electrons by a deep level from a conduction band. The rate of capture of electrons 'R2' is described by

$$R_2 = \sigma_n \langle v_n \rangle_{th} P_T n \qquad (2.2)$$

Where 'n' is the number of electrons in the conduction band. P_T the concentration of empty deep states, 'σ_n' is the capture cross section and $<v_n>_{th}$ the average thermal velocity of the electrons. Essentially an electron with this velocity must come within an area σ_n of the trap to be captured.

Process 3

Emission of holes from a deep level into valance band. The rate of hole emission 'R3' is described by

$$R_3 = e_p p_T \qquad (2.3)$$

Where 'e_p' is the holes emission rate.

Process 4

Capture of holes by a deep level from the valance band. The rate of capture of hole 'R_4' is described by

$$R_4 = \sigma_p \langle V_p \rangle_{th} n_T P \qquad (2.4)$$

Where 'σ_p' is the hole capture cross-section and $<v_p>$ is the average thermal velocity of the holes and 'p' the density of holes in the valance band, respectively. The net rate of electron leaving the conduction band is

$$\frac{-dn}{dt} = \sigma_n \langle V_n \rangle P_T n - e_n n_T \qquad (2.5)$$

Where 'σ_p' is the hole capture cross section and $<v_p>_{th}$ the average thermal velocity of the holes and 'p' the density of holes in the valance band, respectively. And the net rate of holes leaving the valance band is

$$\frac{-dp}{dt} = \sigma_p \langle v_p \rangle_{th} n_T P - e_p p_T \qquad (2.6)$$

Thus the rate at which density of filled traps increases is

$$\frac{dn_T}{dt} = R_1 - R_2 - R_3 + R_4 \qquad (2.7)$$

$$\frac{dn_T}{dt} = \frac{-dn}{dt} + \frac{dp}{dt}$$

Utilizing eq 2.6 and 2.7 in the above eq we have

$$\frac{dn_T}{dT} = \sigma_n \langle v \rangle_{th} p_T n - e_n n_T - \sigma_p \langle V_p \rangle_{th} n_T P - e_p p_T$$

If $N_T = n_T + p_T$ the total density of deep states

$$P_T = N_T - n_T$$

So above eq becomes

$$\frac{dn_T}{dt} = \sigma_n \langle V_n \rangle_{th} n(N_T - n_T) - e_n n_T - \sigma_p \langle V_p \rangle_{th}\ n_T P + e_p (N_T - n_T)$$

$$\frac{dn_T}{dt} = N_T(\sigma_n\langle V_n\rangle_{th} n + e_p) - n_T(\sigma_n\langle V_n\rangle_{th} n + e_n + \sigma_p\langle V_p\rangle_{th} p + e_p)$$

$$\frac{dn_T}{dt} = (nc_n + e_p)N_T - (nc_n + pc_p + e_n + e_p)n_T \qquad (2.8)$$

Here

$$C_n = \sigma_n\langle v_n\rangle_{th}$$

$$C_p = \sigma_p\langle v_p\rangle_{th}$$

are capture coefficients of electrons and holes respectively which describe the rate of capturing of electrons and holes.

Eq 2.6, 2.7 and 2.8 are the kinetic equations which completely describe the electrons and hole densities in conduction and valance bands as well as deep levels in any time [8].

For steady state

$$\frac{dn}{dt} = 0$$

Eq 2.8 becomes

$$(nc_n + e_p)N_T = (nc_n + pc_p + e_n + e_p)n_T \qquad (2.9)$$

2.7 The characteristics of Deep level

The most important parameters of deep levels are:

- Thermal activation energy or enthalpy.
- Binding energy or photo ionization energies.

- Thermal emission rates (e_n, e_p)
- Capture rates/ capture cross-sections (c_n, cp/σ_n,σ_p)
- Concentrations (N_T)
- Temperature dependence of capture cross-sections
- Electric field dependence of thermal emission rates

The most important of these parameters is E_T, The energy position of the deep level inside the forbidden gap. For donor type levels, this is (E_C- E_t) and for acceptor type levels, it is (E_T-E_V), where E_c and E_V are the position of conduction and valance band edges respectively. One can further use these parameters to describe a deep level using their dependence of different physical parameters. For example, activation energy can be field dependent, so can the emission rates. Similarly the temperature dependent capture gives us interesting insight of the phenomena of capture of carriers .

CHAPTER 3

DEEP LEVEL TRANSIENT SPECTROSCOPY

This chapter describes the technique used for the characterization of deep levels namely *Deep Level Transients Spectroscopy* (DLTS).This technique utilized the junction capacitance of a p-n junction and the analysis of deep levels in the space charge region on the basis of Shockley-Read-Hall statistics.

3.1 Introduction

Characterization of a defect is one of the most important processes to obtain excellent semiconductor devices. DLTS is widely used to evaluate electrical properties of a point defect in a semiconductor device with measuring a capacitance transients against a voltage step pulse [5,17].

DLTS can also give the concentrations, energy and capture rates of both kinds of traps. It is spectroscopic in the sense that it can also resolve signals due to different traps. In the many variants of the basic DLTS technique the deep levels are filled with free carriers by electrical or optical methods. Subsequent thermal emission processes give rise to a capacitance transient. The transient is analyzed by signal processing while the temperature is varied at a constant rate. This results in a full spectroscopic analysis of the semiconductor band gap.

For a complete understanding of DLTS we must have some basic knowledge of capacitance transients arising from the depletion region of a p-n junction. The use of capacitance transients for studying the properties of defect centers is well known [6,11]. In usual DLTS measurements, the data analysis should be carried out under the condition that carrier concentration and their depth profile can be regarded as a constant within the observation region.

A brief description of the capacitance change due to the change in occupancy of deep levels in the depletion region is given below.

3.2 p-n junctions Capacitance

In order to understand the effects of trapping and emission of carriers from deep energy levels, which are located in the space charge layer of p-n junction or schottkey barrier, it is important to know the properties of an ideal space charge layer, i.e., without deep levels.

The existence of a space charge layer at a p-n junction or schottkey barrier is a general characteristic of semiconductors. Such a layer is necessary to create electrostatic potential variation needed to counteract the diffusion potential of carriers across the junction and hence equalize the Fermi levels throughout the material. The ideal space charge layer is shown in Fig.3.1. A p-n junction can be regarded as a parallel plate capacitor, for which the capacitance is given by

$$C = \frac{\varepsilon A}{W} \qquad 3.1$$

A= Area of junction

ε = Dielectric constant of semiconductors

W= Width of depletion region

P^+-n step junction is shown in Fig.3.1 in which the depletion region 'W' extends to n-side (i.e. low doped side) of the junction. Then the depletion region width is related to the applied bias as

$$W^2 = \frac{2\varepsilon(V_{bi} + V_R)}{QN_{D,A}} \qquad 3.2$$

V_{bi}= built-in potential

V_R= Reverse bias

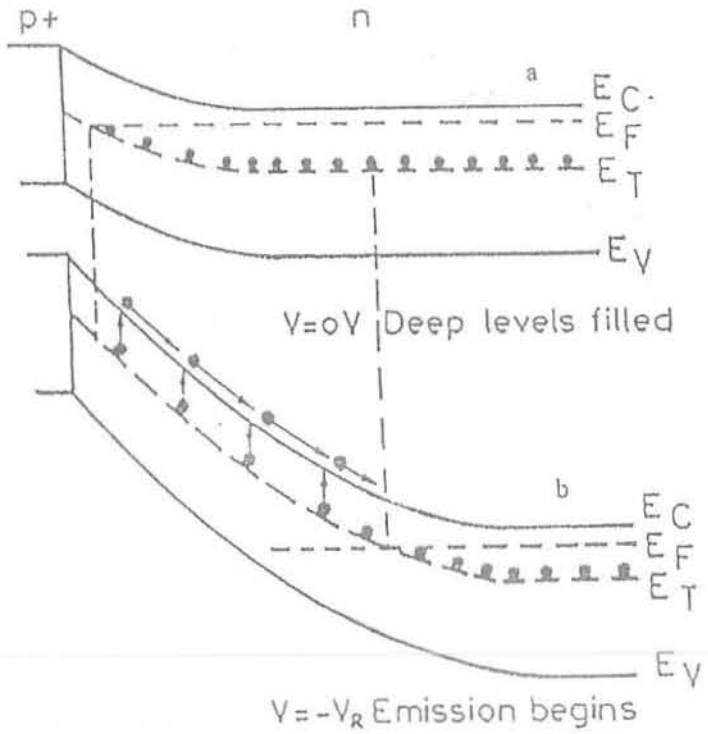

Fig.3.1. Energy band diagram of a p+ -n junction with an electron trap present at energy E_T. (a) the junction at zero applied bias (b) the junction at steady reverse bias V_R.

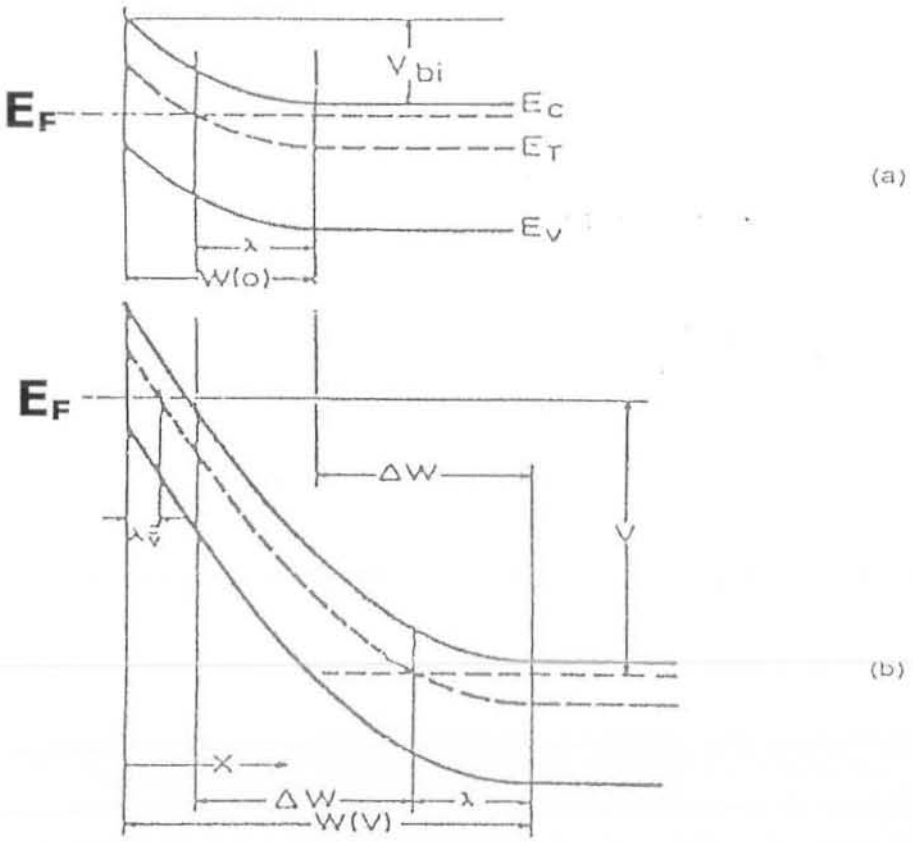

Fig. 3. 2. Energy band diagram of a p+ -n junction illustrating the edge region λ and the corresponding depletion region width at (a) zero applied bias (b) at reverse bias V_R

N_D= Shallow level impurity concentration

The depletion region of one –sided junction can be expressed as

$$\frac{1}{C^2} = \frac{2(V_{bi} + V_R)}{2A\varepsilon qN_{D,A}} \qquad 3.3$$

The plot between $1/c^2$ verses V_R, results in a straight line whose slope gives the shallow impurity concentrations, while the intercept at $1/C^2=0$ yields the built-in voltage of the junction. There are two main features of the space charge layer i.e.,

1. The width of the layer can readily be adjusted by varying the bias voltage.
2. A large varying electric field exists in the space charge even at zero applied bias

A large electric field means that the carriers, thermally emitted from the traps in the space charge layer, are swept out in a very short time, typically 10^{-10} to 10^{-12} seconds. Therefore the retrapping effects can be neglected and the analysis of the thermal emission transients is considerably simplified. Now we will discuss the transients' response of junction capacitance, which will help to understand the DLTS operations.

3.3 Transient Response of junction Capacitance:

In order to explain DLTS we must first consider the more basic problems of capacitance transients, the use of capacitance transients for trap studies in semiconductors is well known [15-4]. This technique is used to obtain information about an impurity level in the depletion region of schottky barrier or a p-n junction by observing the capacitance transient associated with the return to thermal equilibrium of the occupation of level following an initial nonequilibrium condition.

To understand the transient behavior of the junction, we take an example of a p-n junction diode with a deep level defect lying at energy position E_t in the band gap. Under steady state conditions, there is no net flow of the charge carriers at the center

and as the concentration of electrons and holes in the space charge region is negligibly small, we can ignore it. Using these conditions in eq

$$\frac{dn_T}{dt} = \frac{-dn}{dt} + \frac{dp}{dt}$$

We get the following equation that deals with the recombination kinetics

$$\frac{dn_T}{dt} = e_p N_T - n_T(e_p + e_n) = 0$$

$$n_T = N_T\left[\frac{e_p}{e_p + e_n}\right] \qquad (3.4)$$

This eq (3.4) gives the concentration of filled traps 'n_T' under steady state condition. Where $N_T = n_T + p_T$ is the total density of the deep levels and n_T and p_T can be defined as

$$n_t = N_T f \qquad \text{(Filled traps)} \qquad (3.5)$$

Similarly

$$P_T = N_T(1-f) \qquad \text{(empty traps)} \qquad (3.6)$$

Now if we perturb the system by some external means, the system goes to non-equilibrium state and the concentration of the filled traps changes. As a consequence the total charge in the depletion region and capacitance of the junction will change. For simplicity we consider an asymmetric p^+-n junction in which one side is much more heavily doped than the other and depletion region is almost completely on low doped side (i.e. n-side) of the junction as shown in Fig.3.3.Suppose a reverse bias 'v_R' is applied to the sample, and then decreased to zero for a short interval of time by a bias pulse. As a result of the decrease in the depletion region, the electrons from the conduction band will flow to the region that was previously depleted of the carriers and the levels within this region will capture these electrons.

Now, if the temperature is very low, electron re-emission can be neglected and we get the rate equation as

$$\frac{dn_T}{dt} = c_n(N_T - n_T) \qquad (3.7)$$

Where 'c_n' is the electron capture coefficient. If the bias pulse is long enough, then all the trap levels will be filled by electrons i.e. $n_T = N_T$. By the end of the pulse, the sample is returned to the quiescent reverse bias 'V_R' and the depletion region is again depleted of the free carriers. The filled levels start to emit electrons so that the concentration of the filled traps 'n_T' will vary with time and this variation can be expressed by the following equation.

$$\frac{dn_T}{dT} = e_p N_T - n_T(e_p + e_n) \qquad (3.8)$$

The solution of the above equation is given by

$n_T = N_T$ For $t \leq 0$

$$n_T(t) = \left[N_t\left(\frac{e_p}{e_n + e_p}\right) + \left\{ N_t\left(\frac{e_p}{e_n + e_p}\right)\exp\left(-(e_n + e_p)t\right)\right\}\right] \qquad (3.9)$$

From the above equation it is clear that the decrease in the concentration of the filled traps follows an exponential behavior with a time constant 'τ', which is given by

$$\tau = 1/e_p + e_n \qquad (3.10)$$

Considering the deep level to be an electron emitting center i.e. $e_n \gg e_p$, then equation (3.9) becomes

$$n_T = N_T \exp\left[\frac{-t}{\tau}\right] \qquad (3.11)$$

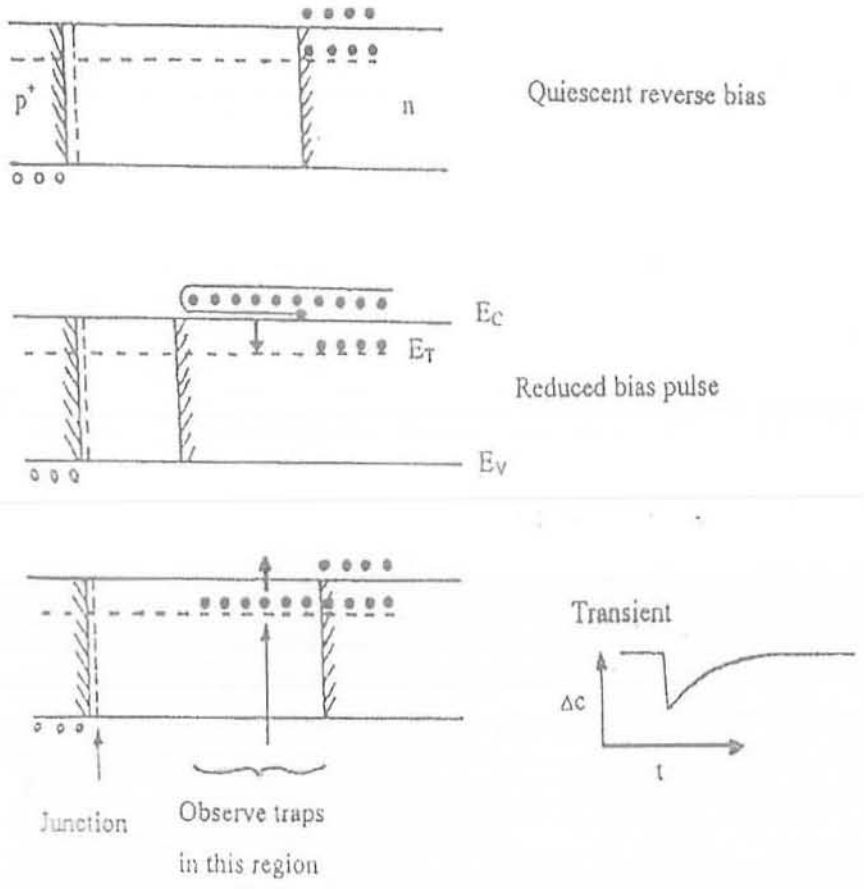

Fig.3.3. Majority carrier pulse for p+ -n junction. Trap occupation and space charge layer width are indicated corresponding to the condition before, during and after the pulse (from top to the bottom of the figure, respectively).

This equation shows that the magnitude of the transient gives an estimate of the density of the deep levels filled with the carriers and the time constant 'ι' gives the emission rate of the electrons, where

$$\tau = \frac{1}{e_n} \qquad (3.12)$$

Since it is difficult to measure the change in the concentration of the filled traps with time, so the simplest indirect method is to measure the capacitance changes of the junction that are related to the concentration variations. The capacitance of a p-n junction is related to 'w' in the same manner as parallel plate capacitor, namely

$$C = \frac{\varepsilon A}{W} \qquad (3.13)$$

For P^+-n junctions including the contributions of the filled traps in the depletion region, the width of the depletion region becomes

$$W^2 = \frac{2\varepsilon(V_{bi} + V_R)}{qN_d^*} \qquad (3.14)$$

where $N_d^* = N_d - n_T$

For $n_T << N_d$ Equation (3.14) can be expanded and we get the expression for the capacitance as

$$C = C_\circ\left[1 - \frac{n_T}{2N_d}\right] \qquad (3.15)$$

Where $C_\circ$ is the capacitance at quiescent reverse bias 'v_R'. Including the variation of n_T with time, we get the time dependence of the capacitance for majority carrier emitters as

$$C = C_\circ\left[1 - \frac{N_T}{2N_d}\exp\left(\frac{-t}{\tau}\right)\right] \qquad (3.16)$$

The change in the capacitance of the junction by the emission of the carriers from trap at constant reverse bias is a parameter to be used in calculating the emission rates and the trap concentration in the space charge region of a p-n junction. These changes are in the form of transients.

3.4. Understanding of the DLTS operations

The physics of the DLTS is capacitance transients out lined in sec.3.3.The capacitance transients of eq 3.16 can be obtained by holding the sample at constant bias and temperature and applying a single filling pulse. The resultant isothermal transient can then be analyzed to obtain the emission rate of the carriers at the particular temperature. For obtaining a wide range of emission rates, this is a time consuming technique. Also if many deep levels are present, the experiment and its analysis become difficult. This is where DLTS has a major edge over the conventional techniques. The essential feature of DLTS is its ability to setup a rate window that is, the rate of change of the capacitance transient in a fixed emission rate window is monitored as the junction temperature varied. This concept is illustrated in Fig.3.4a.The electronic detection system of the deep level transient spectrometer is designed to yield maximum response only within the preselected emission rate window. Instead of talking about rate, we can say that the DLTS, technique uses a time filter which gives an output signal only when a transient has a time constant coinciding with the centre of time window of the filter. A very important property of such a filter (time or rate) is that output is proportional to the amplitude of the transient. There are many ways of constructing a time filter. One of the widely used methods is, in which a variation of the duel-gate boxcar integrator is employed.

It precisely determines the emission rate window and provides signal-averaging capabilities to enhance the signal to noise ratio, making it possible to detect the defect centers having very low concentrations. The use of double boxcar for rate window selection is illustrated in Fig.3.4 b. These transients are fed into the double boxcar with gates set at t_1 and t_2. The difference $C(t_1)-C(t_2) = \Delta C$ is calculated. It is clear from the figure that this ΔC goes through a maximum. This ΔC after going through some filtering is converted into the DLTS output S (T) given by (assuming an exponential transient):

$$S = \Delta C(t_1) - \Delta C(t_2) \qquad (3.17)$$

Where $\Delta C(t_1) = \Delta C_o \exp\left[\frac{-t_1}{\tau}\right]$

And $\Delta C(t_2) = \Delta C_o \exp\left[\frac{-t_2}{\tau}\right]$

Here $\Delta C_o = C(0) - C(\infty)$ is the total change in the capacitance.

Therefore, we can write equation (3.17) as

$$S(T) = \Delta C(0)\left[\exp\left(\frac{-t_1}{\tau}\right) - \exp\left(\frac{-t_2}{\tau}\right)\right] \qquad (3.18)$$

For different rate window (t_2-t_1) corresponding to different emission rates as shown in Fig.3.4c the peak will appear at different temperatures. Using $\frac{ds(T)}{d\tau} = 0$, (at peak position) gives the maximum value of $\tau = \tau_{max}$

$$\tau_{max} = \left[\frac{t_2 - t_1}{\ln\left(\frac{t_2}{t_1}\right)}\right]$$

$$\tau_{max} = \left[\frac{t_1(x-1)}{\ln x}\right] \qquad (3.19)$$

Where $x = \frac{t_2}{t_1}$ .It is evident from the equation (4.19) that t_1 and t_2 can be varied in three ways given below

(a) Fix t_1 and vary t_2

(b) Fix t_2 and vary t_1

(c) Fix t_1/t_2 and vary t_1 and t_2

The shape and amplitude of the DLTS peak changes with the variation of t_1 and t_2 in the first two cases while it does not changes in the third case because t_1/t_2 remains constant so the choice (c) remains constant. So the choice (c) is recommended. Plugging the value of τ_{max} in the expression for S gives S_{max} as

$$S(T)_{max} = \Delta C(0)\left[\exp\left(\frac{-\ln x}{x-1}\right)\right] - \exp\left[\frac{-x\ln x}{x-1}\right] \qquad (3.20)$$

From this above equation, the peak height of the DLTS signal is seen to be independent of the absolute value of t_1 and t_2 rather it depends upon their ratio. In addition, $S(T)_{max}$ is proportional to $\Delta C(0)$ and therefore, to the defect concentration N_t. Hence the DLTS peak height can directly give the defect center concentration.

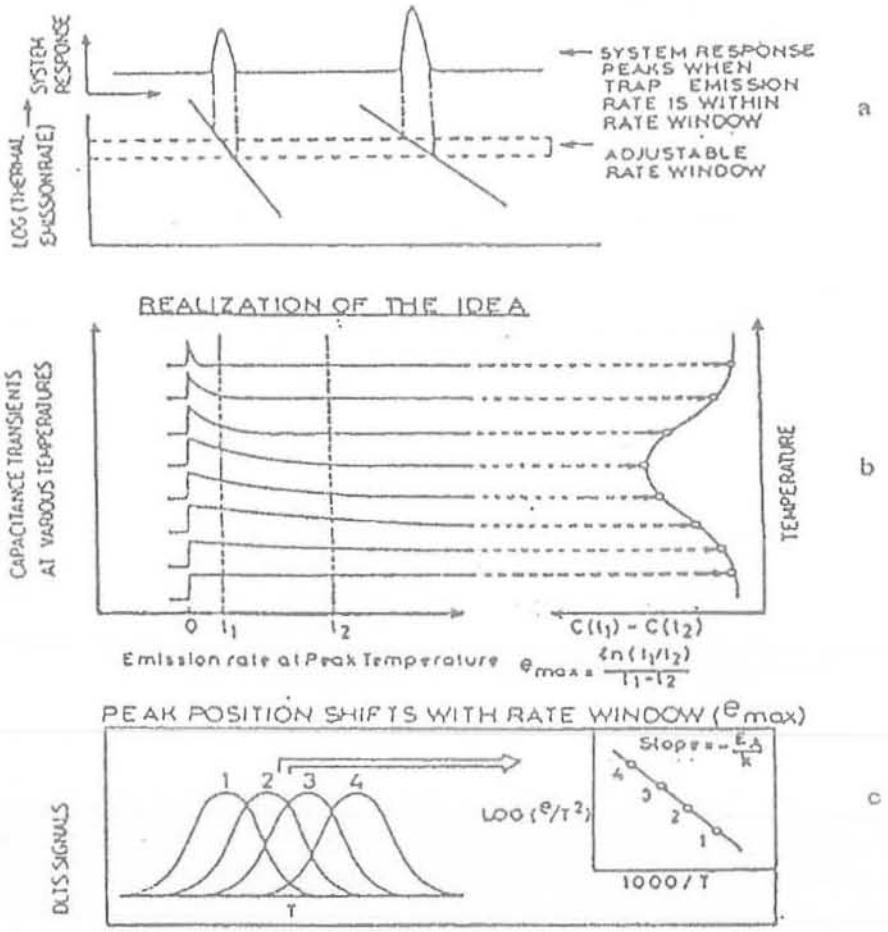

3.4 Diagram illustrated the basic principles of DLTS. (a). the rate window concept, (b). application of rate window concept using a time filter such as dual - gate box car and (c). diagram showing a shift of peak positions in temperature with rate window and arrhenius plot obtain from the peak positions.

3.5 Characteristic of DLTS Measurements

Below are discussed some ways in which the DLTS technique can be used to Study defect centers in semiconductors and to obtain their different characteristic Parameters.

3.5.1 Majority Carrier Emission Rates

Using DLTS technique, majority carrier emission rates can be obtained by applying a sufficiently high reverse bias but less than the break down voltage of the junction, followed by a pulse close to Zero volt. This sequence is repeatedly applied to the sample as depicted in Fig.3.5a. The bands have been assumed to be flat for simplicity. The sample is initially cooled to low temperature so that there is no emission of carriers. During these repeated applied pulses, the levels are filled with majority carriers. As soon as the sample returns to quiescent reverse bias, the level starts emitting and results in a transient. During a transient, the capacitance is measured at the pre-set rate window and DLTS output is plotted as a function of temperature.

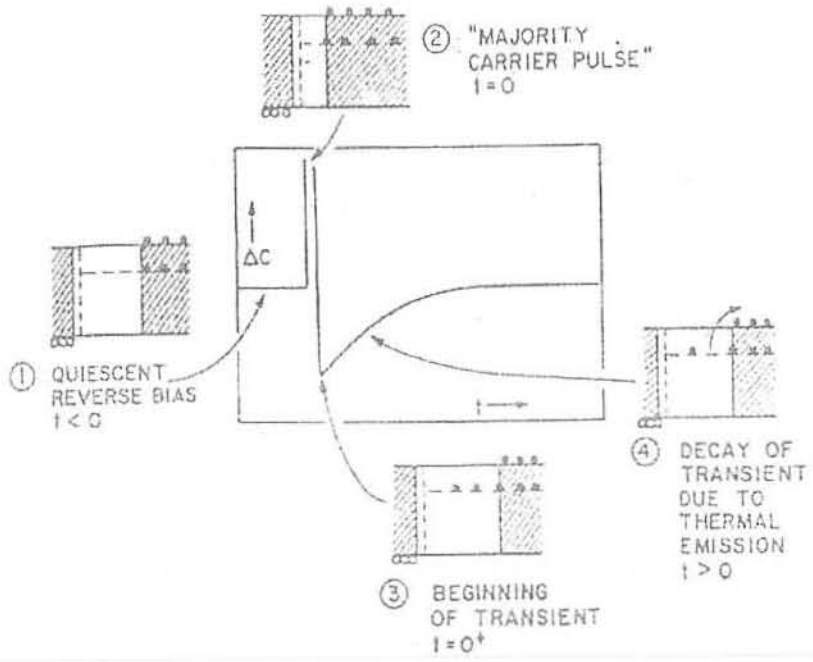

Fig. 3.5. The Isothermal capacitance transient for thermal emission from a majority carrier The inset 1-4 shows trap the condition of the trap occupation, space charge layer width (unshaded) and free carrier concentrations during the various phases of the transient in a p+ -n junction.

3.5.2 Minority Carrier Emission Rates

For observation of minority carriers, we have to first fill the level with minority carriers. This is accomplished through minority carrier injection by forward biasing the diode so that a current flows. After the end of the bias pulse, as the sample returns to the quiescent reverse bias, the deep level will emit minority carriers giving rise to a transient. Thus the DLTS measurement is the same as for the majority carrier emission except that the sign of the peak is now opposite. The pulse and the transient are shown in Fig.3.5b.

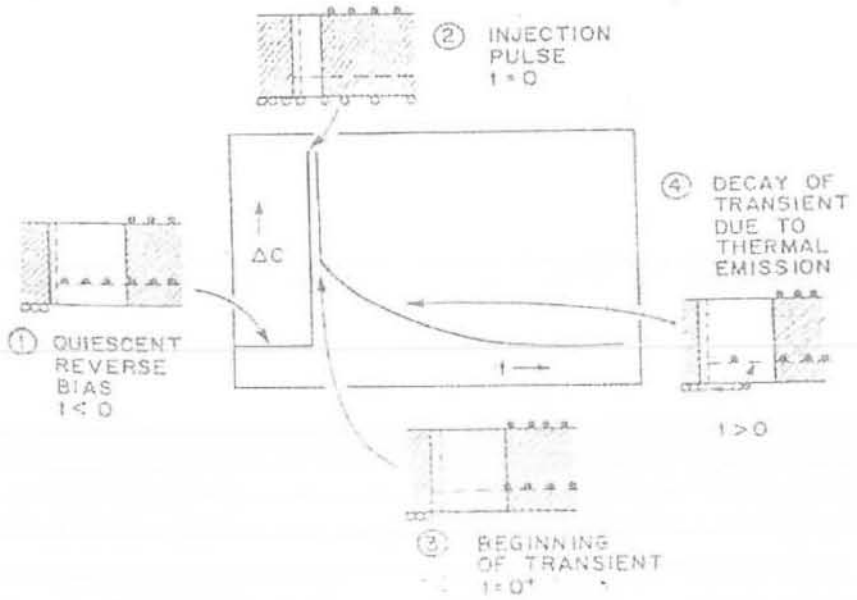

Fig.3.5 b. Isothermal capacitance transient for thermal emission from a minority - carrier trap. The insets 1-4 show the conditions of the trap occupation, space charge layer width (unshaded) and free carrier concentrations during the various phases of the transient in a p^+ - n junction.

3.5.3 Activation Energy

The activation energy (ΔE) of the deep level can be obtained by the slope of an arrhenius plot constructed between different (e_{max}/T^2) and (1/T) values, taking by recording several DLTS scans at different rate windows. Under thermodynamic equilibrium, the emission of carriers from deep level is given by

(i) Electron emission

$$e_n = \frac{1}{\tau} = \sigma_n \langle V_n \rangle_{th} N_c \exp\left[\frac{-\Delta E}{kT}\right] \qquad (3.21)$$

(ii) Hole emission

$$e_p = \frac{1}{\tau} = \sigma_p \langle V_p \rangle_{th} N_v \exp\left[\frac{-\Delta E}{kT}\right] \qquad (3.22)$$

Here $\Delta E = E_c - E_T$ (for electron emission)

$\Delta E = E_T - E_v$ (for hole emission)

and ,(σ_n,σ_p),($\langle v_n \rangle_{th}$,$\langle v_p \rangle_{th}$) and (N_c,N_v) are the capture cross-sections, average thermal velocity and effective density of states in the conduction band and valance band, for electrons and holes, respectively.

The temperature dependence of average thermal velocity and effective density of states can be separated out in the form of factor 'T^2'. Therefore, the substitution of these parameters in terms of temperature yield

$$e_{n,p} = AT^2 \exp\left[\frac{-\Delta E}{kT}\right] \qquad (3.23)$$

Where $A = \langle V_{n,p} \rangle_{th} N_{c,v} \sigma_{n,p}$ (the temperature independent part)

$$\ln\left[\frac{e_{n,p}}{T^2}\right] = \ln A + \left[\frac{-\Delta E}{kT}\right] \qquad (3.24)$$

The plot of ln $[e_{n,p}/T^2]$ versus [1/T] gives a straight line whose slope gives the activation energy and the capture cross-section can be calculated by the intercept at ($T=\infty$). The value of the capture cross-section which is obtained by this method is normally different from actual value, but this value provides information about capture properties of deep levels.

3.5.4 Deep level Concentration

The peak height of a DLTS scan is proportional to the number of the emitted carriers from the deep level at that temperature. The emission of charge carriers from the depletion region gives rise to change in capacitance of diode. This change in capacitance 'ΔC' is proportional to the number of emptied deep levels given by the following equation,

$$\frac{\Delta C}{C} = \frac{N_T}{2N_d} \qquad (3.25)$$

3.5.5 Capture Cross-section

The capture cross-section of a carrier is a measure of how close an electron and hole has to come to the level to be captured and provides inside about the electronic structure of the deep level center and the defect lattice interaction. One can extrapolate the Arrhenius plot to (1/T) and obtain the capture cross-section at $T=\infty$ from the intercept. But this usually leads to far from true of the capture cross-section because of the following reason:(i) $\sigma_{n,p}$ may be temperature dependent and hence the extrapolation is not valid.(ii) a slight error in the extrapolation may leads to several order of magnitude difference in value of capture cross section. Hence, capture cross-section must be directly measured over as long a range of temperature as possible.

To measure the capture cross section directly we select a rate window and DLTS scans are carried out while the filling pulse width is varied for each scan. The peak height varies with varying the pulse width until it reaches its maximum value when all the centers are filled. Such a pulse is called saturation pulse.

The peak height is related to filling pulse t_p via the following equation.

$$1-\frac{S}{S_\infty}=\exp\left[\frac{-t_p}{\tau}\right] \qquad (3.26)$$

Where 's' is the peak height for any pulse width t_p and 's_∞' is the saturated peak height. The slope of ln [1-S/S_∞] versus t_p gives [1/τ]

σ_∞ can then be calculated using the equation given below.

$$\sigma_n=\left[\frac{1}{\pi n\langle V\rangle_{th}}\right] \qquad (3.27)$$

The capture cross-section can be calculated by plugging the values of 'n' and $\langle v_n\rangle_{th}$.

CHAPTER 4

EXPERIMENTAL DETAILS

Introduction

This chapter gives the detail of the samples used for the experiment, their growth, and experimental setup, outlines the experimental procedure and measurement carried out for the characterization of various deep level parameters.

4.1 Sample used for Experiment

The sample used in this experiment consist of Indium Phosphide which is Iridium doped. The sample is fabricated by the Metal Organic Chemical Vapour Deposition Technique (MOVCD) also known as Metalorganic vapour phase epitaxy (MOVPE). It is a chemical vapour deposition method of epitaxial growth of materials, especially compound semiconductors from the surface reaction of organic compounds or metal organics and metal hydrides containing the required chemical elements. Indium Phosphide is grown in a reactor on a substrate by introducing Trimethylindium ($(CH_3)_3In$) and Phosphine (PH_3) as shown in fig 4.1.Transport of precursor molecules i.e ($(CH_3)_3In$) and Phosphine (PH_3) is by carrier gas N_2 or H_2 on to a heated substrate. Formation of the epitaxial layer occurs by final pyrolysis of the constituent chemicals at the substrate surface. In contrast to molecular beam epitaxy (MBE) the growth of the crystals is by chemical reaction and not by physical deposition. This takes place not in a vacuum, but from the gas phase at moderate pressures (2 to 100 kPa).

We have doped the sample with Iridium using the precursors cyclopentadienyl-bis-ethene-irridum [1].

The principal of MOVCD technique is introduced as follows. Atoms of different elements are combine together with complex organic gas molecules and passed over a hot semiconductor wafer. The heat breaks up the molecules and deposits the desired atoms on the surface of wafer, layer by layer. We can change the properties of crystal grown at almost atomic level by varying the composition of the metal-organic gas.

It can grow high quality semiconductor thin layers, as thin as millionth of a millimeter and crystal structure of these layers is perfectly aligned with that of the substrate.

4.2 Growth of n-type samples

Our sample consists of p^+-n junctions grown by Low-Pressure Metal Organic Chemical Vapour deposition (LP-MOVCD). The substrate used was a 350μm thick n^+-InP layer doped with Si. On the top of this substrate used was a 3μm thick n-InP: Si layer. The sample had a typical background donor doping of 3×10^{15}-$5\times10^{16}cm^{-3}$. The top most p^+-InP layer consists of approximately 0.7μm thick InP:Zn. Nitrogen or Hydrogen was used as the carrier gas for transporting the metal organics and the growth was carried out at a typical temperature and pressure of 640C°and 20mbar, respectively.

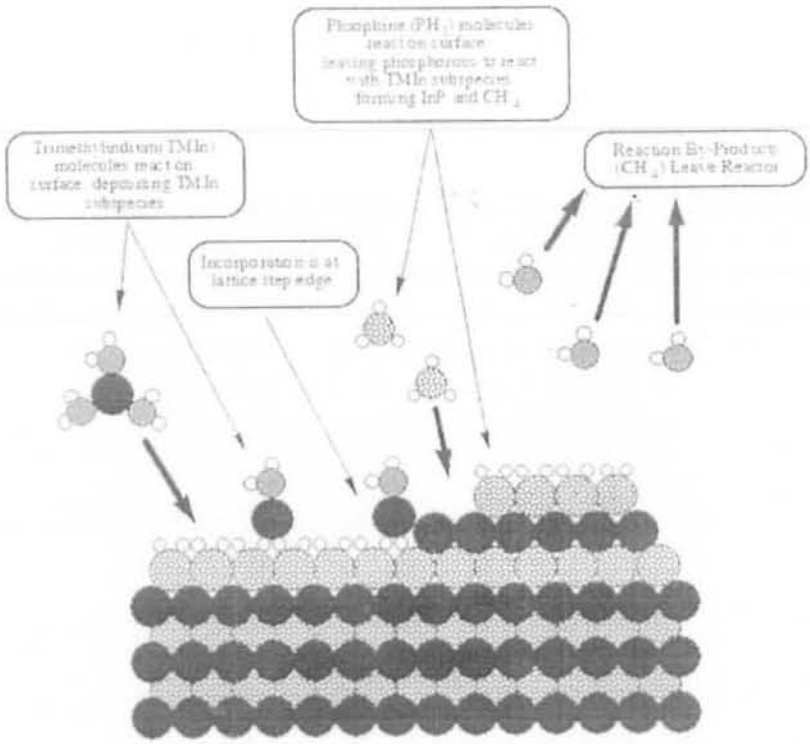

Fig. 4.1 Growth of Indium Phosphide by MOVCD

4.4 Current-Voltage Characteristics

Current voltage (I-V) characteristics are very important in DLTS measurement. An I-V measurement of the pn-junction gives information of the consistency and quality of samples for further measurement and analysis. The selection of suitable samples for DLTS measurements was carried out on the basis of leakage currents of the pn-junction. A digital electrometer has been used to measure the leakage current of the pn-junction. From I-V measurements we calculate the maximum reverse bias that can be applied to the pn-junction. This meter can measure the leakage current of the pn-junction up to 1pA. Such samples were chosen for which the leakage current of the pn-junction is less than 0.1μA. at a suitable reverse bias. Block diagram of the set-up for I-V measurements is shown in Fig. 4.2.

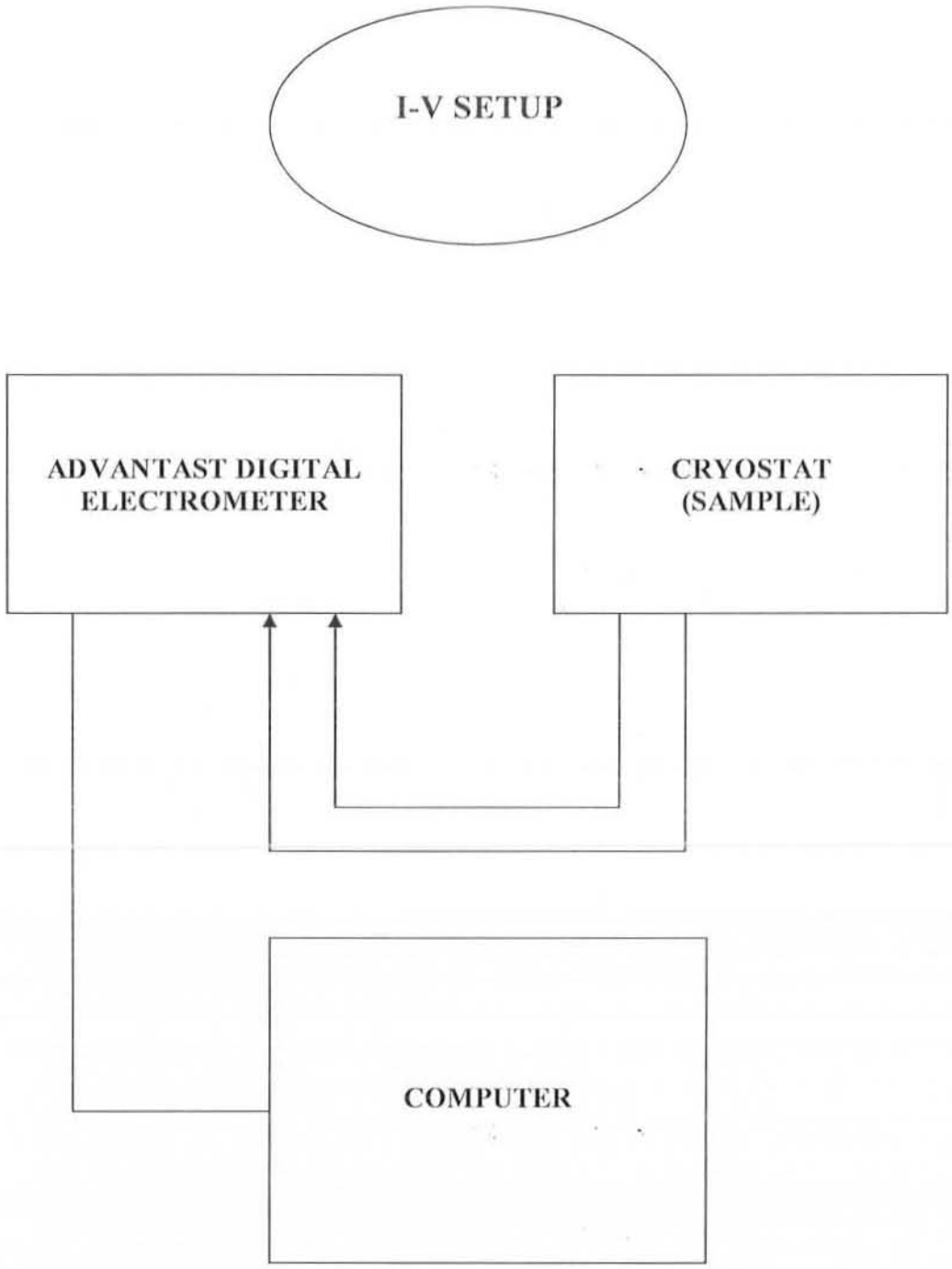

Fig. 4.2. I-VSETUP

4.5 Capacitance –Voltage Characteristics

Capacitance-Voltage (C-V) characteristics provide very important information about the pn-junction. To study the pn-junction it is necessary to have knowledge of its shallow level doping concentration, shallow level doping profile and built-in voltage. C-V measurements provide this information. A C-V plot gives the following information about the parameters that are very important in analyzing the DLTS results.

i) Types of pn-junction whether it is abrupt ($1/C^2$ varies linearly with the applied reverse voltage V_r) or linearly graded ($1/C^3$ vs. V_r results into a straight line.)

ii) Built-in voltage, V_{bi} of the pn-junction.

iii) Concentration of the shallow dopands N_d

N_d or N_a can be calculated by the slope of the C-V plot by the following calculations.

$$\text{Slope of C-V plot} = \frac{d}{dv_r}\left[\frac{1}{c^2}\right] = \frac{2}{\varepsilon_s e A^2 N_{A,d}}$$

Where e is the charge on the carrier and A is the area of the pn-junction.

Therefore,

$$N_{d,a} = \frac{2}{\varepsilon_s e A^2}\frac{d}{dv}\left[\frac{1}{C^2}\right]^{-1}$$

We take C-V plots from computer.

4.6 DLTS Measurements

A 1 MHz DLTS system, DLS-81 made by Metrimpet, Hungary based on lock-in frequency principal, was used for DLTS measurements. It is equipped with two

built-in pulse generators for applications such as deep level profiling or double pulse excitation. The repetition rate of the excitation pulses can be varied from 0.1 HZ to 1 KHz. For accurate measurements of the repetition rate and biases, a digital oscilloscope, National VP-5740A was used.

A Leybold Heraeus 57550 digital frequency counter was used to measure the accurate emission rate window. The system has the ability of applying the maximum reverse bias of 20V. The DLS-81 output signal was plotted on a National VP-6423A X-Y Recorder.

The samples were mounted in a VPF-700 cryostat manufacture by a Janis Research Company U.S.A. It is a versatile variable temperature system that enables sample temperature to be accurately controlled in between 77K and 700K. It has a chromel-Alumel thermocouple to measure the sample temperature. The sample temperature was controlled by a Lakeshore 330 temperature controller. The block diagram of experimental setup is shown in Fig .4.3.

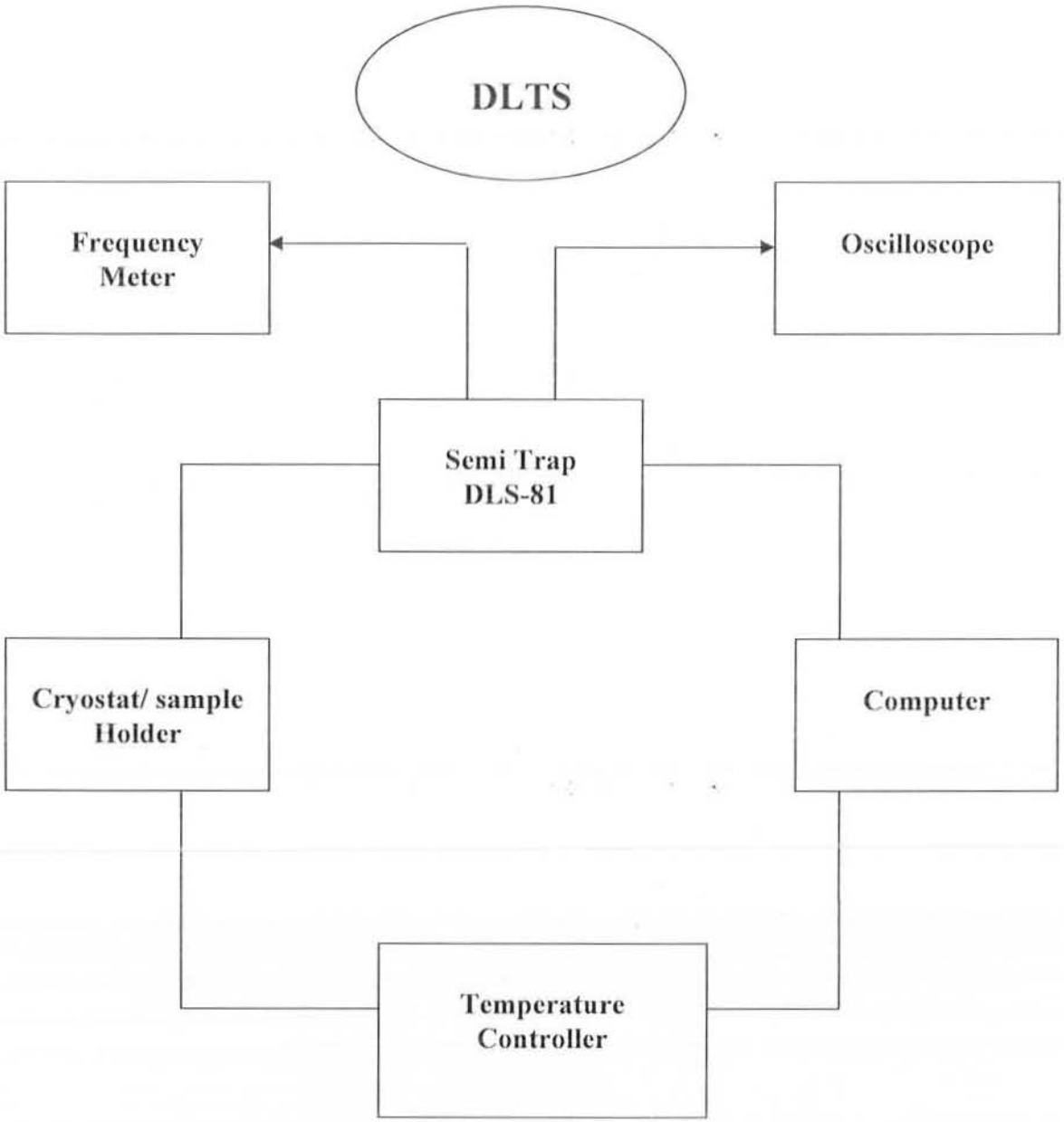

Fig.4.3.DLTSSetup

CHAPTER 5

RESULTS AND DISCUSSION

This chapter describes the results and discussion of the work reported in this thesis. DLTS technique has been used to study the deep levels in InP which is Iridium doped.

First of all the basic measurements Current-Voltage (I-V) and Capacitance Voltage (C-V) were performed to measure the suitability of the sample. The DLTS of the samples were done to characterize the related defects and parameter in the observed peaks in the DLTS spectra.

Current-Voltage measurements have been performed to check the suitability of the pn-junctions. These measurements are carried out in the temperature range from 40K to 320K. Those pn-junctions were selected for which the leakage current was very small. The pn-junction with less than 0.1μA leakage current at the required range of the reverse voltage V_r were selected for DLTS measurements to get meaningful results.

Capacitance-Voltage measurements were carried out on the sample in the temperature range from 40K to 320K. These measurements were necessary to determine the nature of pn-junctions as well as to determine the shallow level concentration and built in voltage. The reverse bias was varied in range 0 to 5V and the corresponding capacitance was recorded.

After performing I-V and C-V measurements, DLTS measurements were carried out on the sample. These measurements were carried out to determine the deep levels introduce in the pn-junction. The DLTS scans repeated at different emission rate windows to obtain a data for calculation of the energy position of the traps in the band gap. Emission rates were measured in the temperature range from 20K to 320K. The maximum emission rates were plotted against the temperature (K) on the semi-logarithmic scale using the eq

$$\ln\left[\frac{e_n}{T^2}\right] = \ln A + \left[\frac{-\Delta E}{K_b T}\right]$$

The slope of the best fit line of the Arrhenius plot, $\ln[e_n/T^2]$ vs. 1000/T gives activation energy of the deep levels. This emission rate of different levels was plotted on semi logarithmic graph .The activation energies are obtained from the best-fit line. Capture cross section σ_∞ for the corresponding levels are calculated from the intercept of $\ln [e_n/T^2]$ vs 1000/T.

5.1 I-V Measurements

We take I-V measurements in the temperature range from 40K to 320K. The setup for I-V measurement is given in Fig. 4.3. The I-V plots are shown in Fig 5.1.

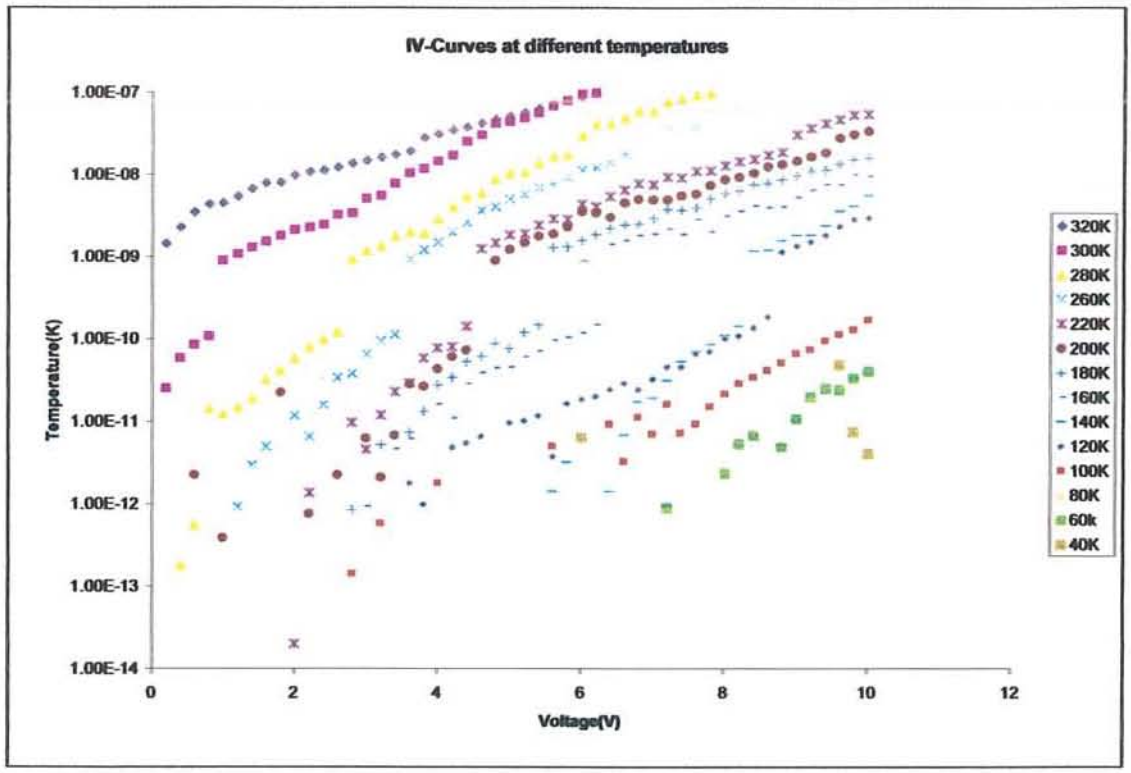

Fig .5.1 IV- Curves at different temperatures

5.2 CV Measurements:

We take CV measurements in the temperature range 40K to 320K. The CV plots are shown in Fig.5.2.

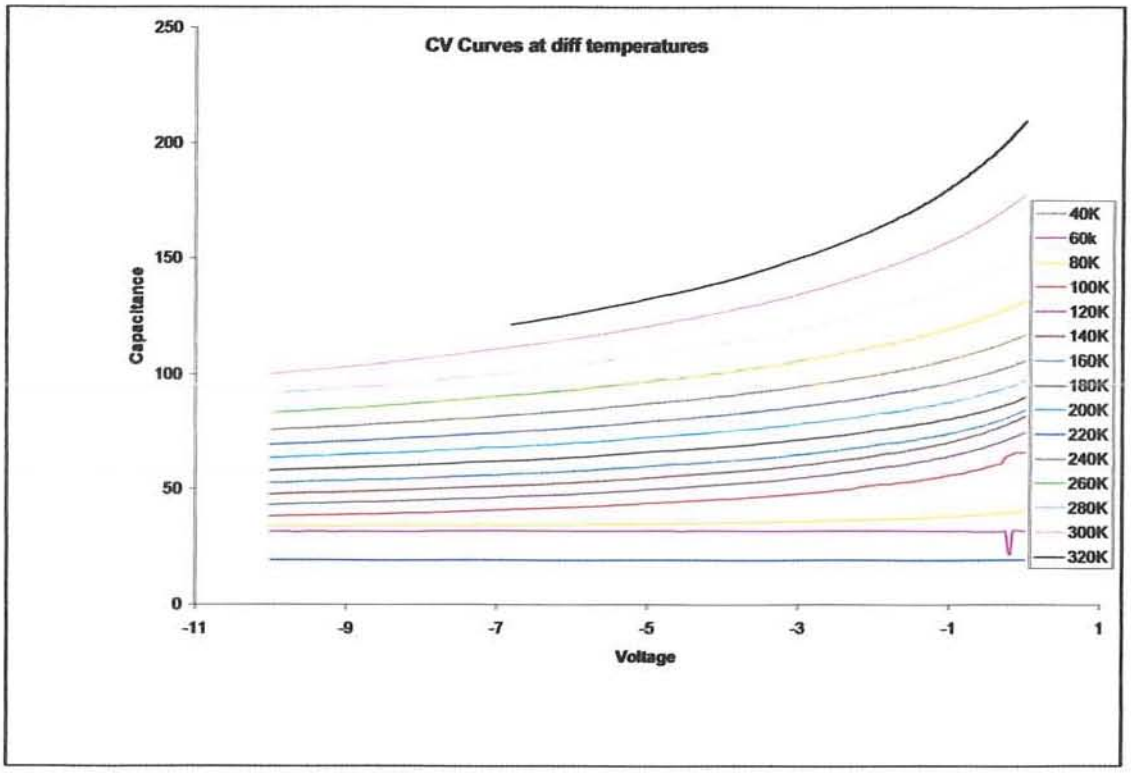

Fig.5.2 CV Curves at Different Temperature.

5.2 DLTS measurements

After performing I-V and C-V measurements, DLTS measurements were carried out on the pn-junction. These measurements were done to characterize the deep levels introduced in the pn-junction.

(a) Majority (Electron Emission) DLTS spectrum

Fig.5.3. shows the typical DLTS majority scan of n-type InP. This DLTS spectrum is taken at -5 volts with 500μsec filling pulse at 101.75Hz (corresponding to an emission rate of 225.95sec^{-1}) from 35K to 325K. A sequence of peaks labeled P0-P5 appeared. The Arrhenius plots of these levels are given in Fig.5.3.

(b) Minority (Hole Emission) DLTS spectrum

Fig.5.4.shows the typical DLTS minority carrier emission scan using injection pulse of 2.25v. This DLTS spectrum is taken at 500μsec filing pulse at 101.75 Hz frequency (corresponding to an emission of 225.95sec^{-1}) from 35K to 325K. Here no minority level appears as shown in Fig.5.4.

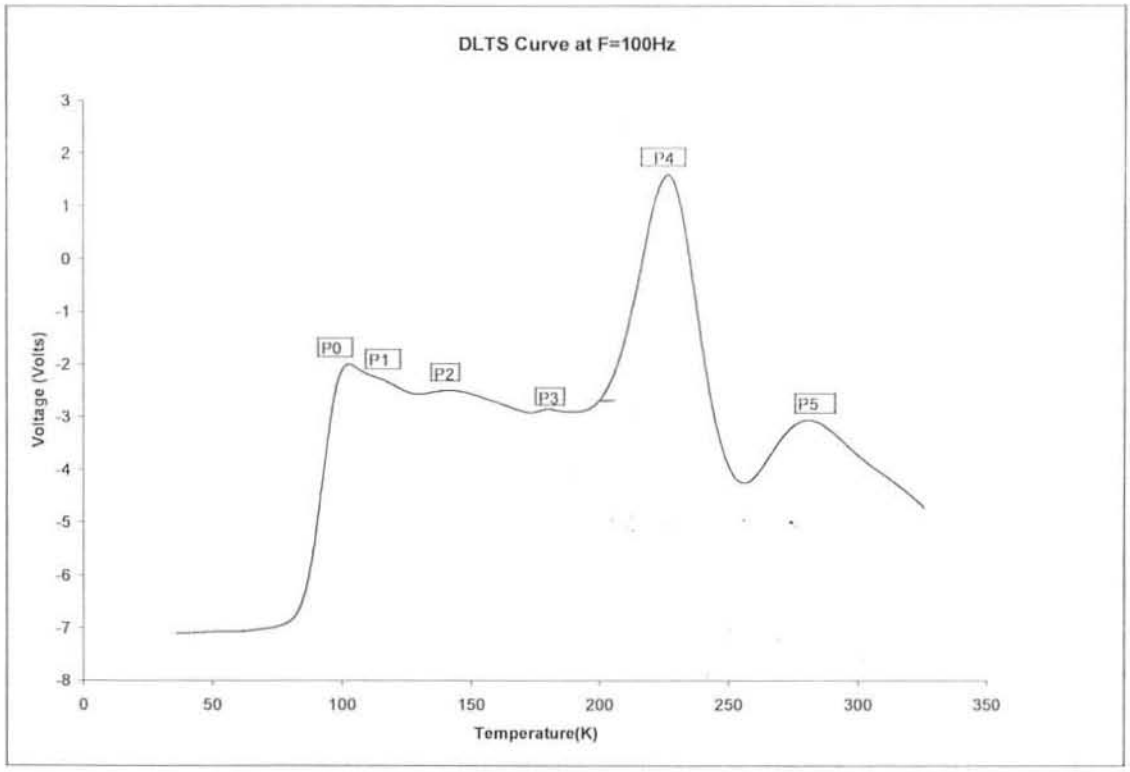

Fig. 5.3 Majority scan at f=101.75 Hz and pulse width 500μs

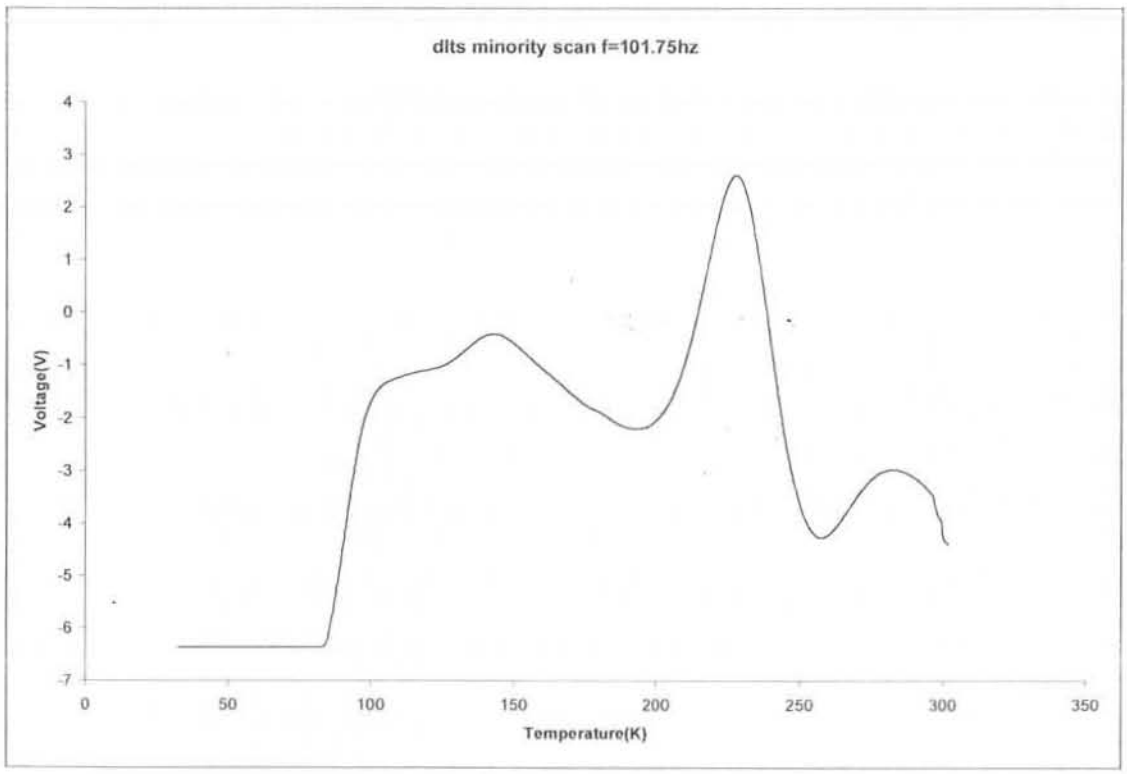

Fig. 5.4 Minority scan at f=101.75 Hz and pulse width 500 μs

5.3 Activation energies of peaks at pulse width 500micsec

In order to find the position of peaks P0-P6 in the band gap, it is necessary to find their activation energy. The e_n/T^2 versus 1/T data has been plotted on a semi-log scale to give the Arrhenius plots for P0-P6 as shown in Fig5.5. To find out their activation energy, several DLTS scans have been carried out at different emission rate windows to obtain a set of emission rate (e_n) at the peak temperature (T) data as shown in. 5.6a, 5.6b, 5.6c, 5.6d, 5.6e, 5.6f, 5.6g, 5.6h.

The peak P0 is overlap of two peaks, one with activation energy 0.22eV with error ±0.02 and other with activation energy 0.09eV with error ±0.04 as shown in Fig.5.6a. The peak P1 is overlap of two peaks, one with activation energy 0.28eV with error ±0.03 and other with activation energy 0.19eV with error ±0.02 as shown in Fig.5.6b.These peaks are due to different emission rate windows. The peak P2 is also overlap of two peaks one with activation energy 0.41eV with error ±0.09 and the other with activation energy 0.22eV with error ±0.01 as shown in Fig.5.6c. The straight line cannot pass from the data points of P2' so its activation energy cannot be found as shown in Fig.5.6d. The activation energy of P3 is 0.38eV with error ±0.02. The activation energy of P4 is 0.53eV with error ±0.02, P5 is 0.51eV with error ±0.004 and P6 is 0.52eV with error ±0.001.

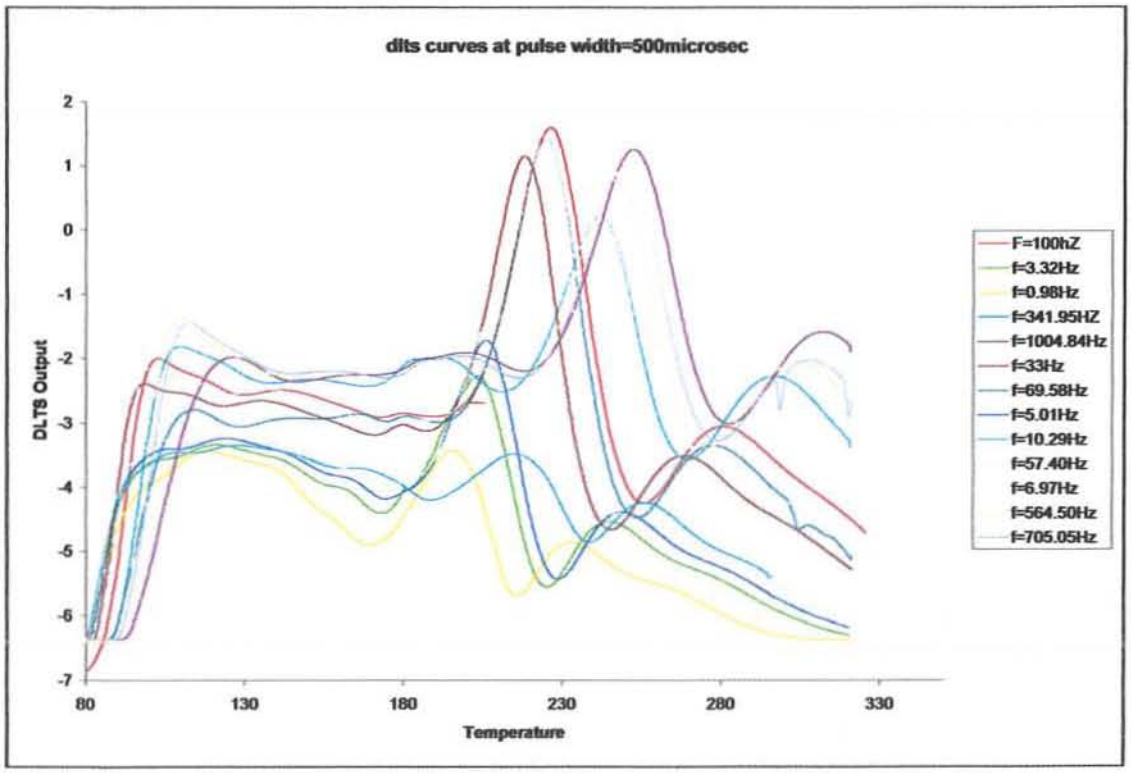

Fig. 5.5 DLTS curve at different frequencies with pulse width 500 μs

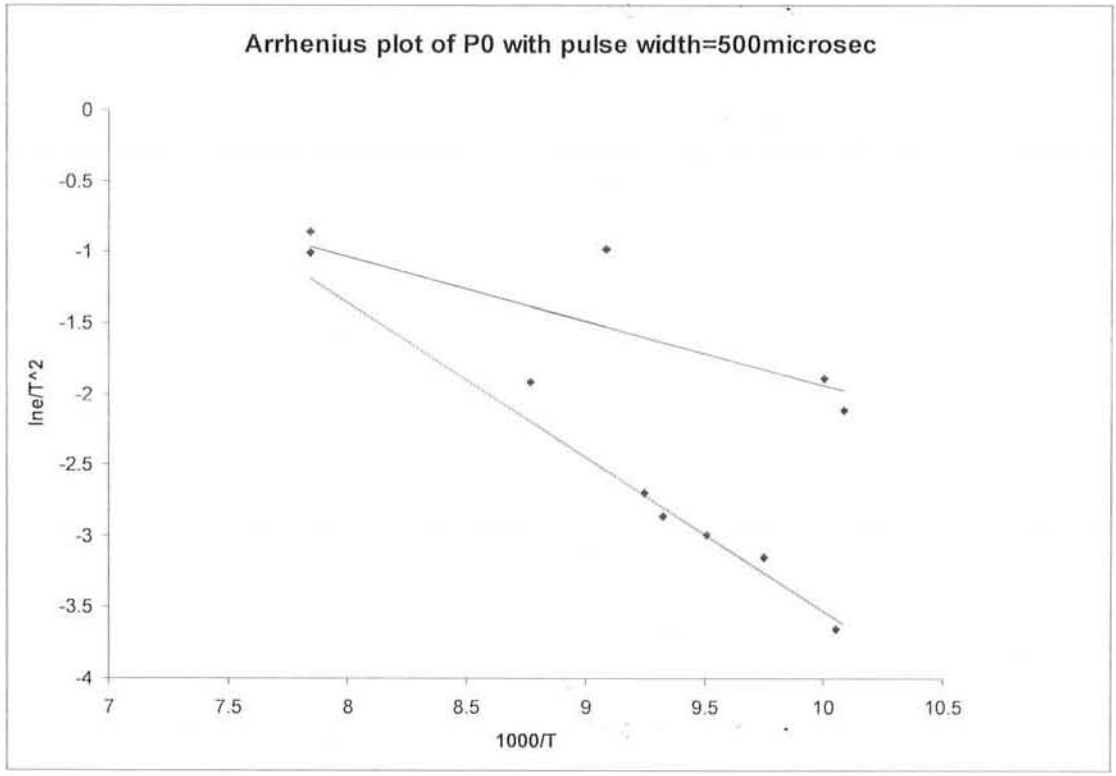

Fig.5.6a Arrhenius plot of P0 with pulse width=500μsec.

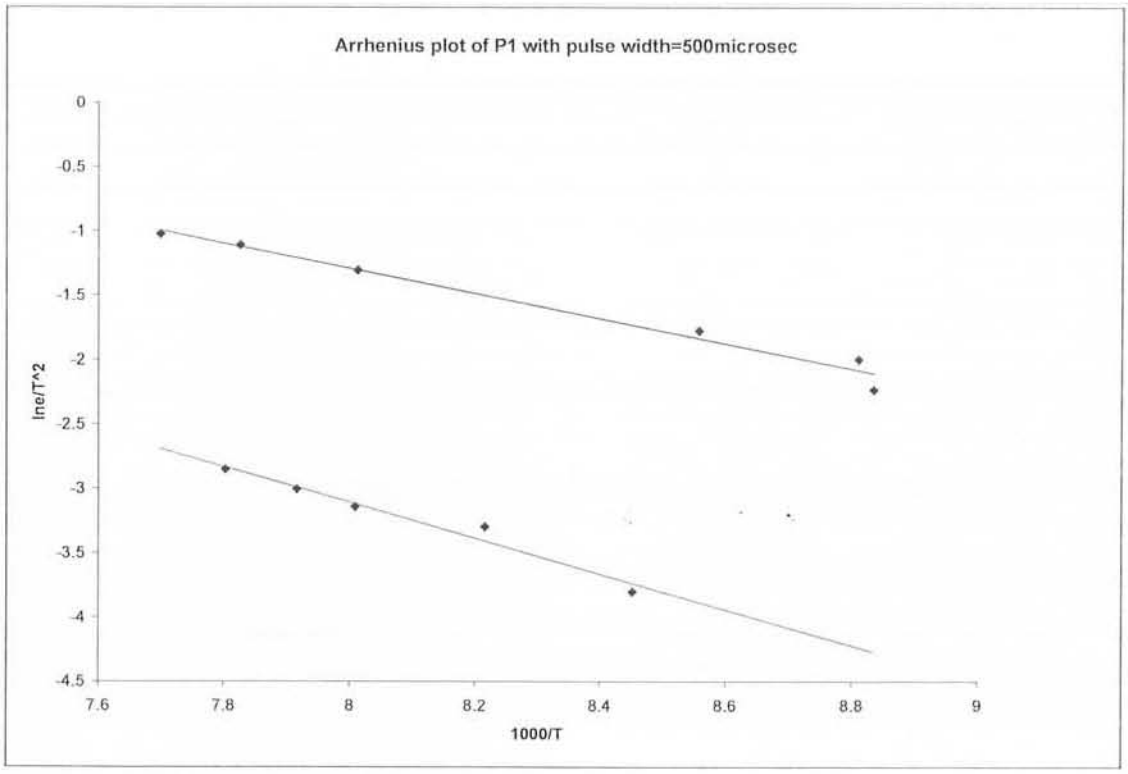

. Fig.5.6b Arrhenius plot of P1 with pulse width=500μsec.

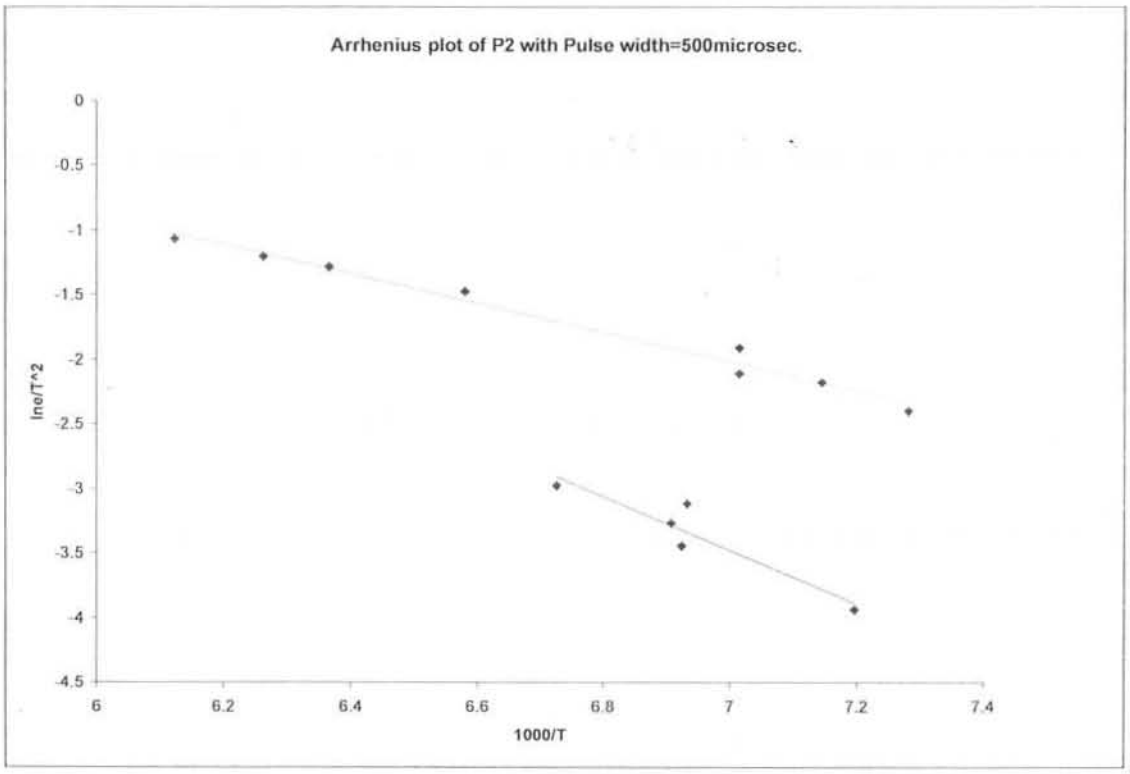

Fig .5.6c Arrhenius plot of P2 with pulse width=500μsec.

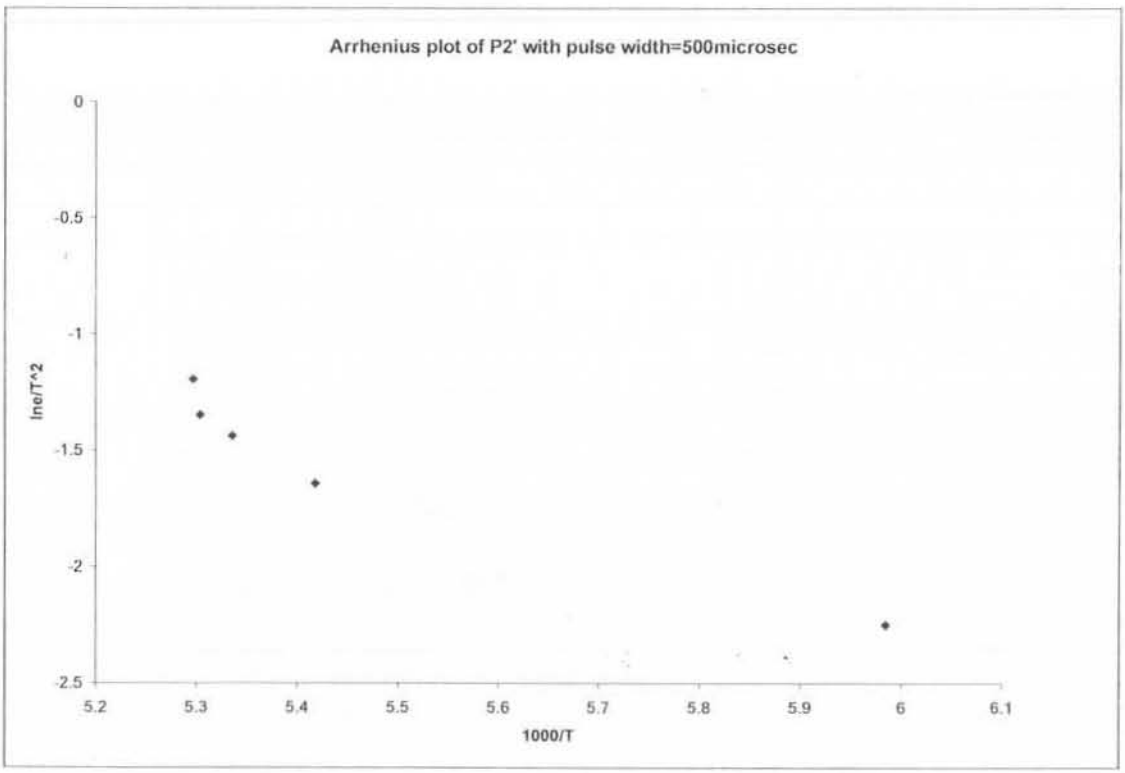

Fig.5.6d Arrhenius plot of peak P2′with pulse width=500μsec

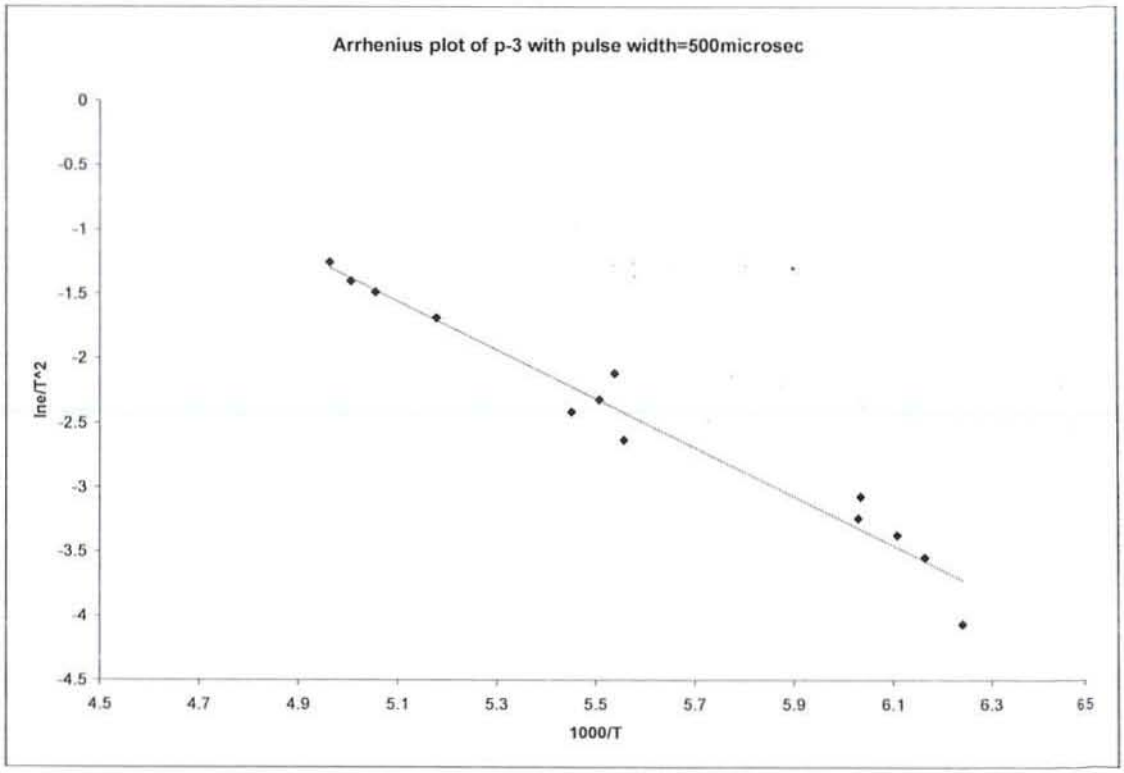

Fig.5.6e Arrhenius plot of P-3 with pulse width=500μsec

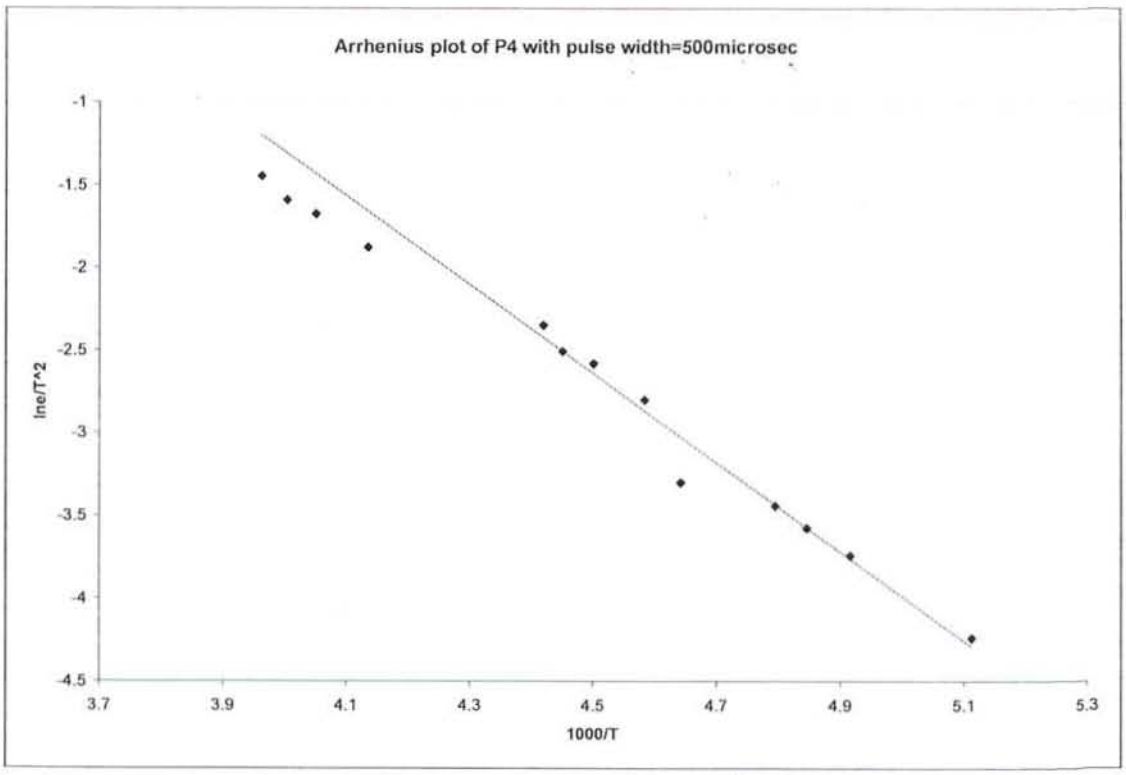

Fig.5.6f Arrhenius plot of P4 with pulse width=500μsec

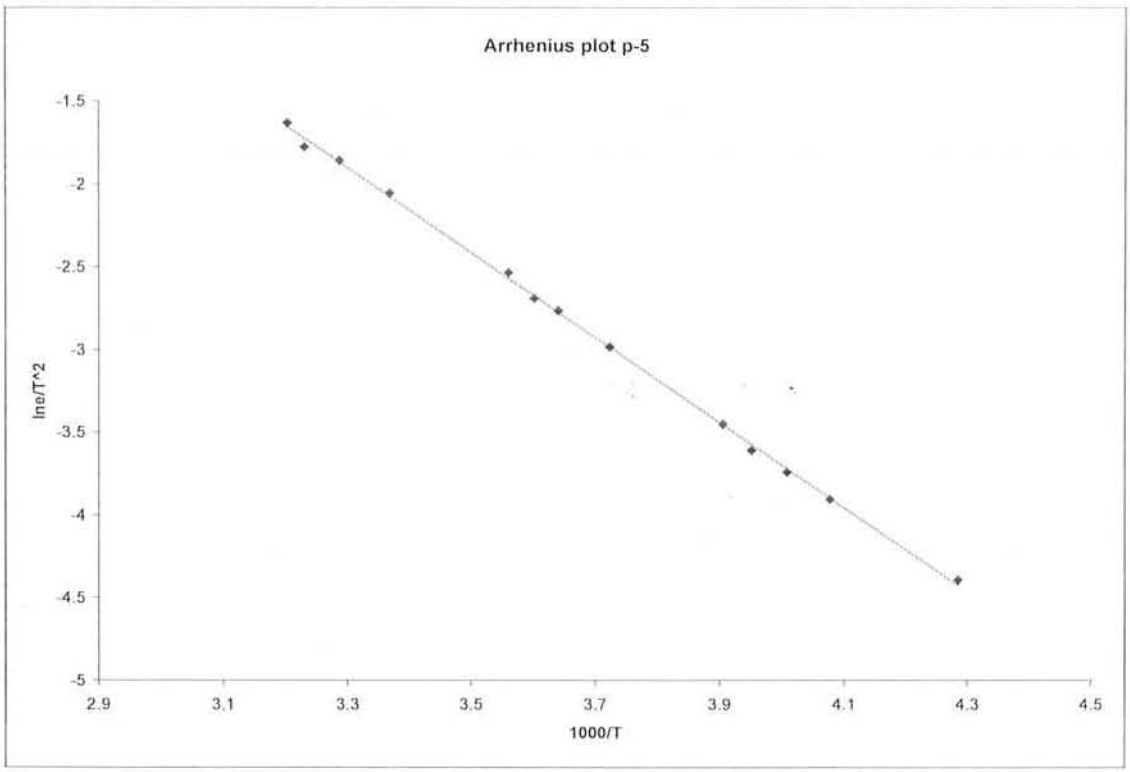

Fig. 5.6g Arrhenius plot of P-5 with pulse width =500μsec

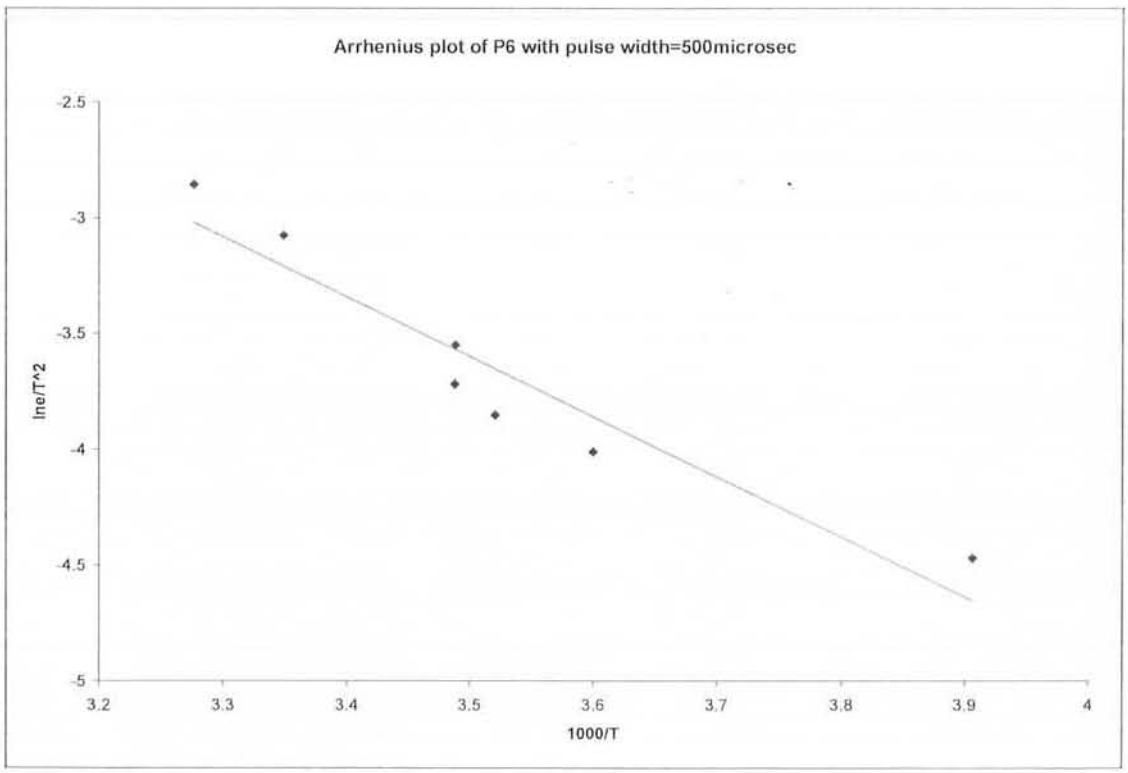

Fig. 5.6h Arrhenius plot of P6 with pulse width =500μsec

4 Activation energies at pulse width 0.5μsec

In order to find activation energies at pulse width 0.5μsec several DLTS scans were carried out at different emission rate windows to obtain a set of emission rate (e_n) at the peak temperature (T). The DLTS spectrum is obtained at -5v reverse bias with 0.5μsec pulse width at different frequencies. The sequence of peaks labeled P0-P4 has been obtained. The DLTS spectrum is shown in Fig. 5.7.

The activation energy for P0 is 0.19eV with error ±0.01, P1 is 0.14eV with error ±0.03, P2 is 0.26 with error ±0.01, P3 is 0.39eV with error ±0.04, and P4 is 0.30ev with error ±0.01. The Arrhenius plots of these levels are shown in Fig. 5.8a,5.8b,5.8c,5.8d,5.8e.

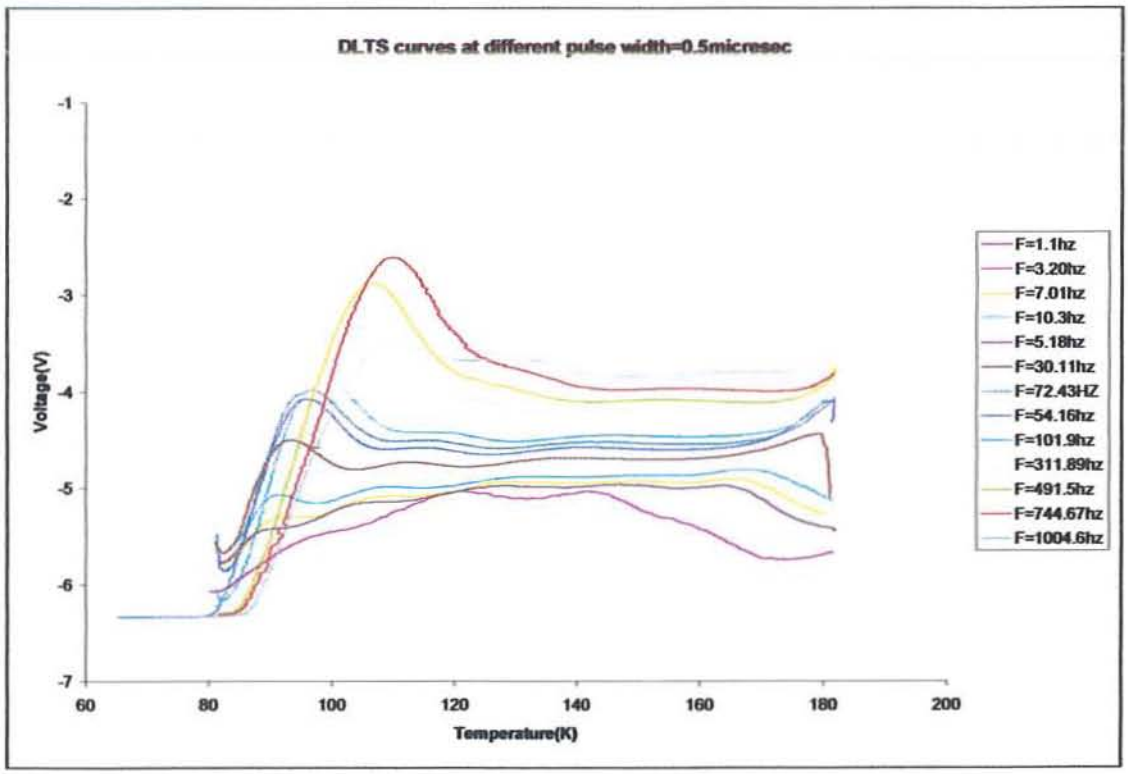

Fig 5.7 DLTS Curve at different frequencies with pulse width =0.5μsec

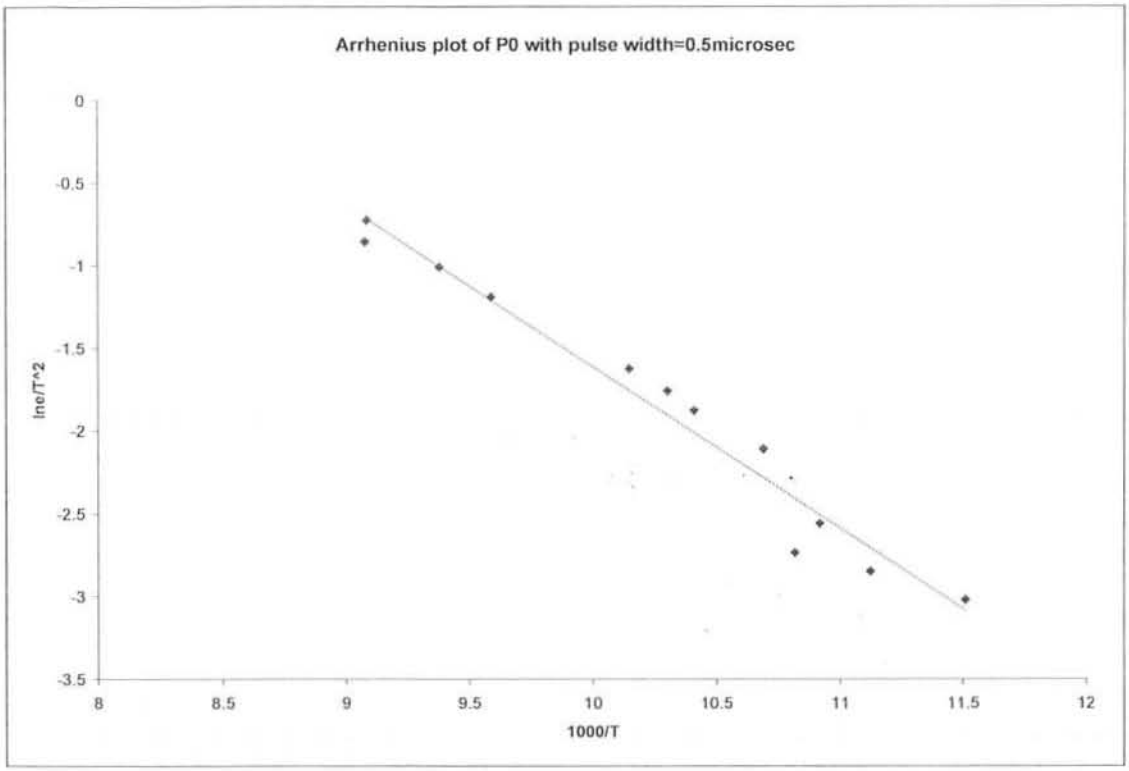

Fig 5.8a Arrhenius plot of P0 with pulse width=0,5µsec

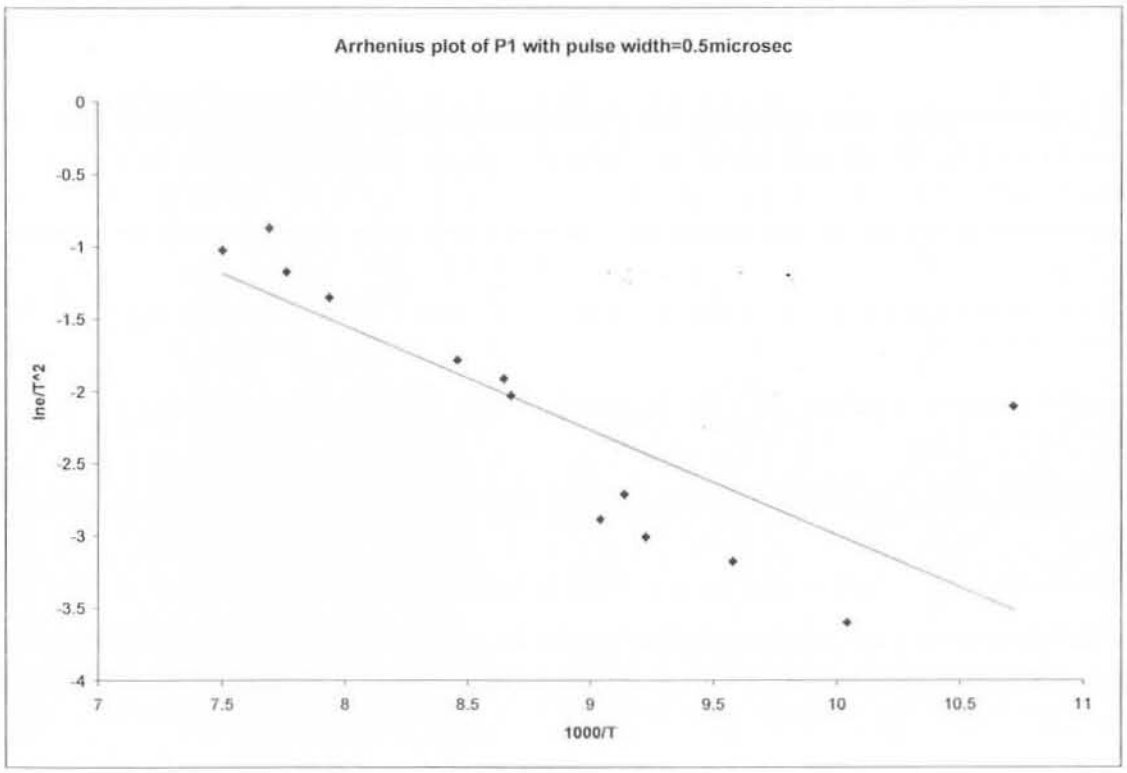

Fig . 5.8b Arrhenius plot of P1 with pulse width=500µsec

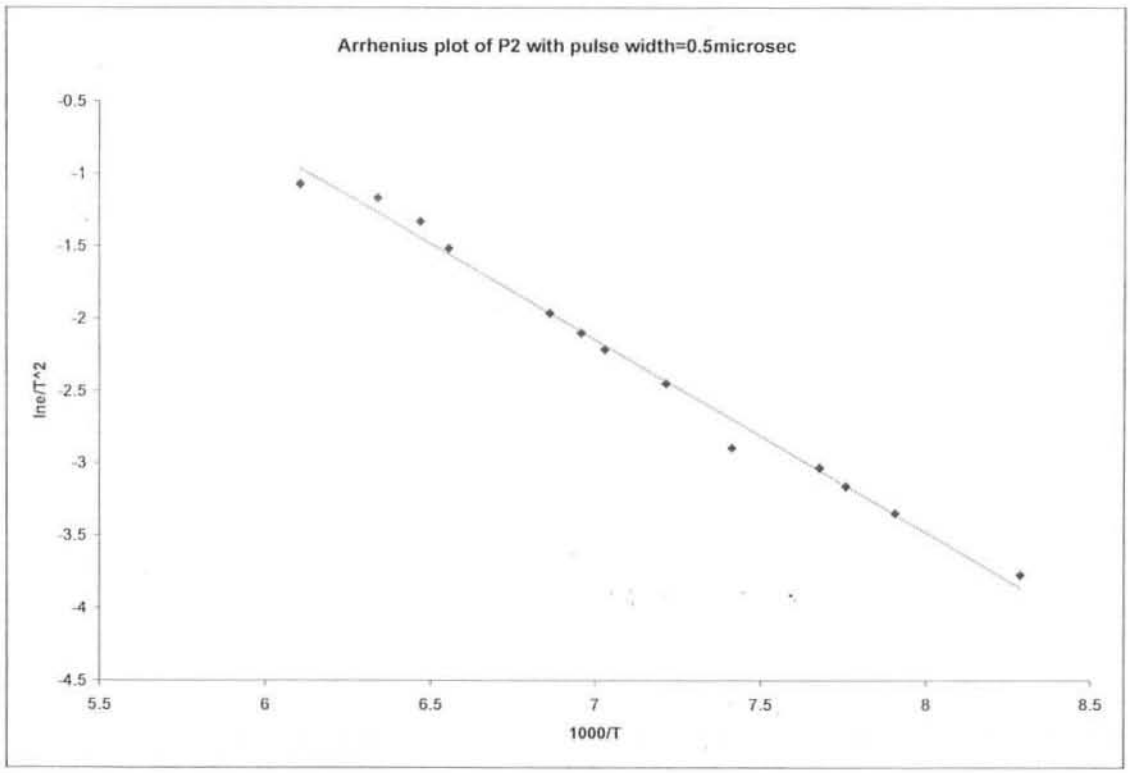

Fig. 5.8c Arrhenius plot of P2 with pulse width=0.5μsec

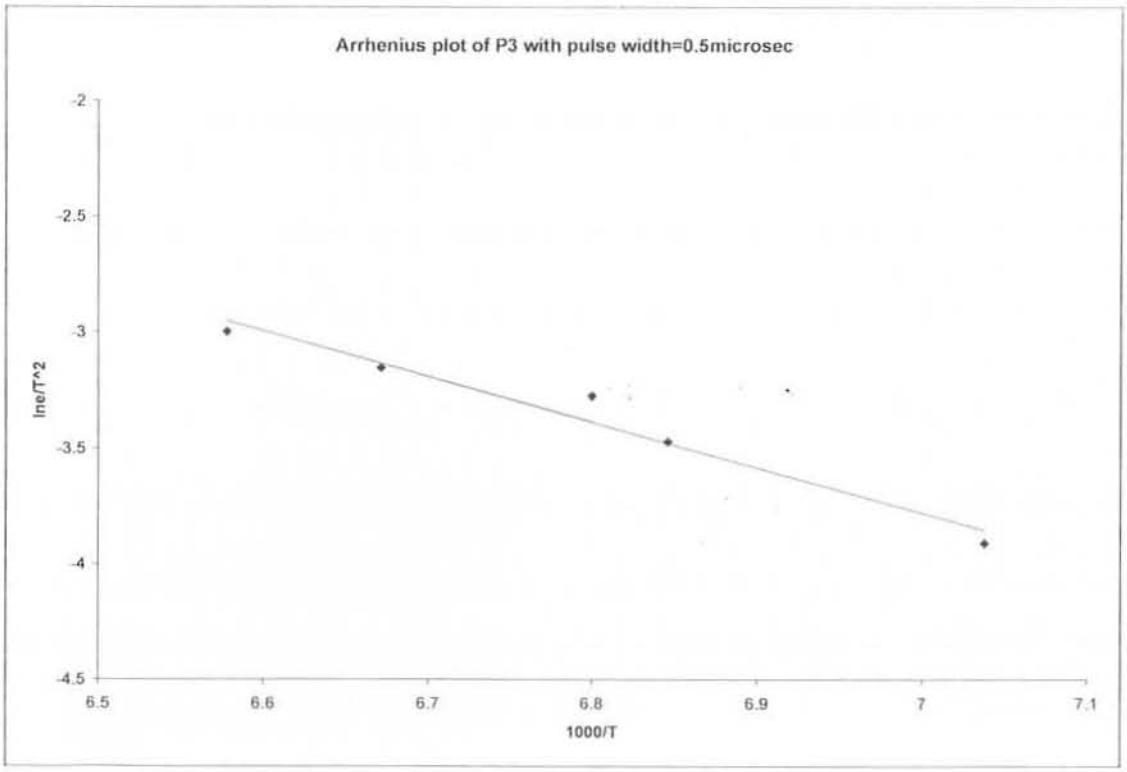

Fig .5.8d Arrhenius plot of P3 with pulse width=0.5μsec

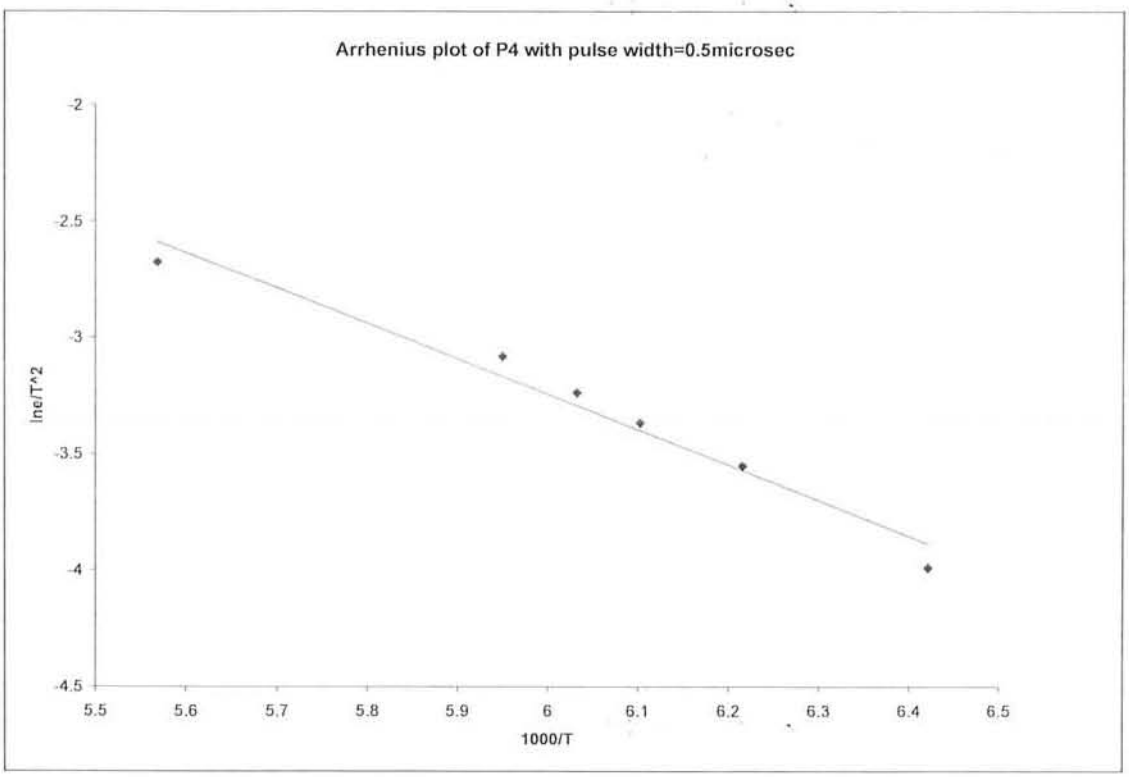

Fig .5.8d Arrhenius plot of P4 with pulse width=0.5μsec

5.5 Capture cross section of highest two levels at 500μsec pulse width

The capture cross section measurements are carried out in the sample on the two dominant peaks P_4 and P_5. The technique is to keep the emission rate fixed and take different scans changing the filling pulse width t_p for each scan. The resulting peak heights S are measured until the peak height is saturated to a value S_∞. The graph is plotted between ln (1-S/S∞) versus t_p. The slope of ln (1-S/S_∞) versus t_p gives $1/\tau$.

Now $\sigma_n=1/(\tau n<v_{th}>)$

The data for P_4 shows a sum of two exponentials giving two values of capture cross section $\sigma_1= 2.19\times10^{-23}cm^2$ and $\sigma_2=1.41\times10^{-20}cm^2$ as shown in Fig .5.9. The two values of capture cross section shows that probably two levels are included.

The data for P_5 shows the sum of three exponentials giving three capture cross sections $\sigma_1 =1.97\times10^{-22}cm^2$, $\sigma_2=6.64\times10^{-21}cm^2$ and $\sigma_3=8.56\times10^{-19}cm^2$ as shown in Fig.5.10.The three values of capture cross section shows that probably three levels are included.

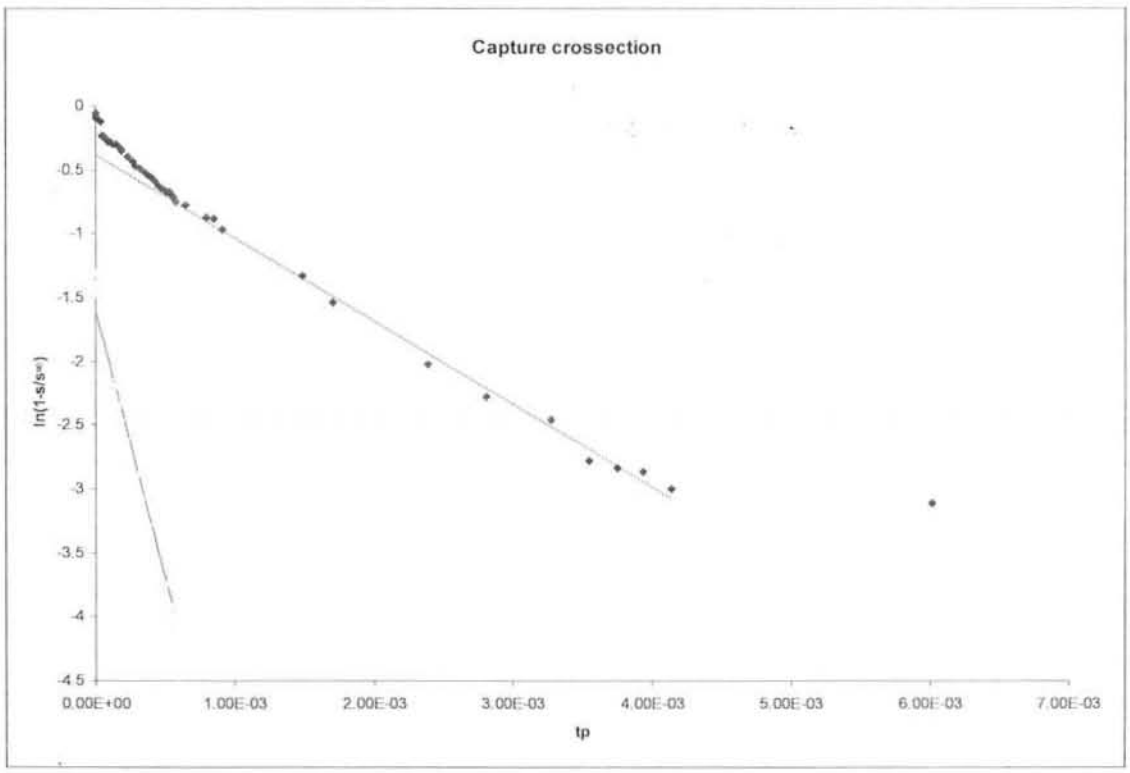

Fig 5.9 Capture cross section of P4

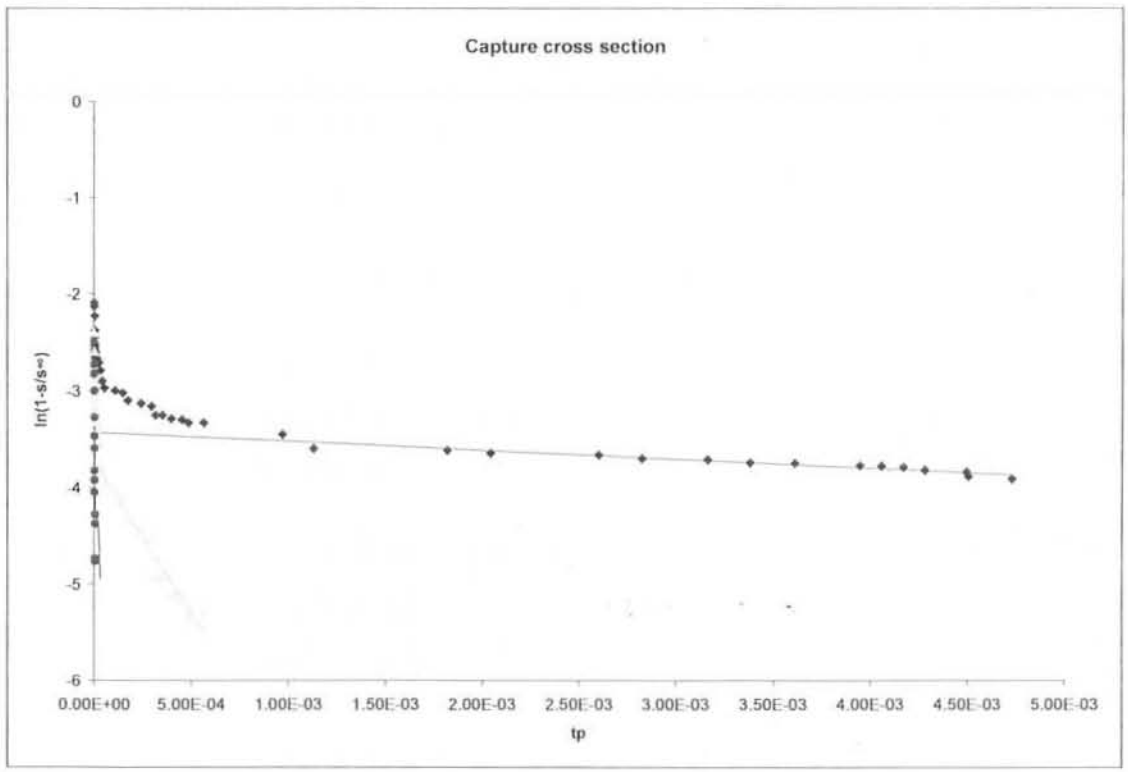

Fig 5.10 Capture Cross Section of P5

CONCLUSIONS

We have presented the study of deep level defects in Iridium doped Indium Phosphide using DLTS technique. On the basis of our investigation in the studies we conclude:

Seven electron emitting deep levels in Iridium doped Indium Phosphide at 500μsec pulse width are obtained. P0 is overlap of two peaks, one with activation energy 0.22eV with error ±0.02 and other with activation energy 0.09eV with error ±0.04. P1 is also overlap of two peaks, one with activation energy 0.28eV with error ±0.03 and other with activation energy 0.19eV with error ±0.02. P2 is overlap of two peaks one with activation energy 0.14eV with error ±0.09 and other with activation energy 0.22eV with error ±0.01. The activation energy of P3 is 0.38eV with error ±0.02, P4 is 0.53 with error ±0.02, P5 is 0.51eV with error ±0.004and P6 is 0.52eV with error ±0.001.

Deep levels are also studied at pulse width of 0.5μsec. The number of peaks decreases with decreasing the pulse width. The activation energy for P0 is 0.19eV with error ±0.01, P1 is 0.14eV with error ±0.03, P2 is 0.26eV with error ±0.01, P3 is 0.39eV with error ±0.04, and P4 is 0.30eV with error ±0.01.

Capture cross section of highest two levels are also found. The data for P4 shows a sum of two exponentials giving two values of capture cross section $\sigma 1 = 2.19\times10^{-23}cm^2$ and $\sigma 2 = 1.41\times10^{-20}cm^2$.

The data for P5 shows the sum of three exponentials giving three capture cross sections $\sigma 1 = 1.97\times10^{-22}cm^2$, $\sigma 2 = 6.64\times10^{-21}cm^2$ and $\sigma 3 = 8.56\times10$-19cm2.

FUTURE WORK

We have observed six majority carrier deep levels in n^+P InP. The future work is required to be done on P^+n InP. Also we can study the behaviour of n^+P InP. Also one can study the behaviour of n^+P InP after annealing and irradiation in future.